

# Connecting Prompt and Afterglow GRB emission

## I. Investigating the impact of optical selection effects in the $E_{\text{pi}} - E_{\text{iso}}$ plane

D. Turpin<sup>1,2,\*</sup>, V. Heussaff<sup>1,2</sup>, J.-P. Dezalay<sup>1,2</sup>, J.-L. Atteia<sup>1,2</sup>, A. Klotz<sup>1,2</sup>, and D. Dornic<sup>3</sup>

<sup>1</sup> Université de Toulouse; UPS-OMP; IRAP; Toulouse, France – e-mail: damien.turpin@irap.omp.eu

<sup>2</sup> CNRS; IRAP; 14, avenue Edouard Belin, F-31400 Toulouse, France

<sup>3</sup> Aix Marseille Universit, CNRS/IN2P3, CPPM UMR 7346, 13288 Marseille, France

Received september 5, 2014; accepted ...

### ABSTRACT

**Context.** Measuring GRB properties in their rest-frame is crucial to understand the physics at work in gamma-ray bursts. This can only be done for GRBs with known redshift. Since redshifts are usually measured from the optical spectrum of the afterglow, correlations between prompt and afterglow emissions may introduce subtle biases in the distribution of rest-frame properties of the prompt emission, especially considering that we measure the redshift of only one third of Swift GRBs.

**Aims.** In this paper we study the brightness of optical GRB afterglows and the role of optical selection effects in the distribution of various intrinsic properties of GRBs and on the  $E_{\text{pi}} - E_{\text{iso}}$  relation discovered by Amati et al. (2002, A&A, 390, 81).

**Methods.** Our analysis is based on a sample of 85 GRBs with good optical follow-up and well measured prompt emission. 71 of them have a measure of redshift and 14 have no redshift. We discuss the connection between the location of GRBs in the  $E_{\text{pi}} - E_{\text{iso}}$  plane and their optical brightness measured two hours after the trigger in the GRB rest frame.

**Results.** We show that the brightness of GRBs in our sample is mainly driven by their intrinsic luminosity and depends only slightly on their redshift. We also show that GRBs with faint afterglows are preferentially located in the upper part of the  $E_{\text{pi}} - E_{\text{iso}}$  plane. This optical selection effect favors the detection of GRBs with bright afterglows located below the best fit  $E_{\text{pi}} - E_{\text{iso}}$  relation whose redshift is easily measurable.

**Conclusions.** The distributions of prompt GRB properties in the rest frame undergo selection effects due to the need to measure the redshift from the optical afterglow emission. These biases put significant uncertainties when interpreting the statistical studies of GRB properties in the rest frame. We show that the  $E_{\text{pi}} - E_{\text{iso}}$  relation is not immune to these selection effects. The difficulty to measure the redshifts of GRBs located far above the best fit  $E_{\text{pi}} - E_{\text{iso}}$  relation may partly explain the observed lack of GRBs with large  $E_{\text{pi}}$  and low  $E_{\text{iso}}$ . However, we observe that bright GRBs may indeed follow an  $E_{\text{pi}} - E_{\text{iso}}$  relation. Studying these selection effects could allow us to better understand the properties of GRBs in their rest frame and the connection between the prompt and the afterglow properties.

**Key words.** gamma-ray bursts – cosmology – redshift

### 1. Introduction

Gamma-ray bursts (GRBs) are cataclysmic explosions resulting from the collapse of massive stars or the merging of two compact objects, see Kumar & Zhang (2014) and references therein. During these events an ultra relativistic jet is produced accompanied by an intense gamma-ray flash which can be seen at very high redshifts (up to  $z=9$  for GRB090429B, see Cucchiara et al. (2011b)). The entire gamma-ray emission is produced in only few seconds (prompt emission) with a total energy released up to  $E \sim 10^{54}$  erg assuming an isotropic emission. This prompt emission is followed by a long lasting and fading multi-wavelength emission from X-rays to radio (afterglow emission) attributed to the external shock between the relativistic ejecta and the interstellar medium (ISM). The origin of the prompt  $\gamma$ -ray emission has been suggested to be due to internal shocks between shells moving at different Lorentz factors,  $\Gamma$ , inside the jet, see (Rees & Meszaros 1994; Paczynski & Xu 1994; Piran 1999; Kumar & Zhang 2014). However, the physical processes at work in these shocks are still not well understood due to strong uncertainties

on the physical conditions (baryon loading, energy dissipation in the jet, acceleration mechanism), see the review by Kumar & Zhang (2014). On the contrary, the afterglow emission is better understood and can be explained by the synchrotron emission from the accelerated electrons in front of the shock between the relativistic ejecta and the ISM (forward shock), (see Sari et al. (1998) & Granot & Sari (2002)). An optical/radio flash is also expected and sometimes observed from a reverse shock propagating into the relativistic ejecta, see (Meszaros & Rees 1993; Kobayashi 2000). In this framework, the dynamics of the afterglow is determined by the microphysics of the shocked material, the ISM properties and the kinetic energy of the blast wave,  $E_k$  which depends on the prompt emission properties (the isotropic gamma-ray energy released,  $E_{\text{iso}}$  and the gamma-ray radiative efficiency,  $\eta$ ). Moreover, studying the optical flash radiation from the reverse shock is a very interesting opportunity to bring constraints on the magnetization parameter of the ejecta (Zhang & Kobayashi 2005; Narayan et al. 2011), the Lorentz factor of the jet, and also on the jet composition (McMahon et al. 2006; Nakar & Piran 2004). Understanding of the connection between the prompt and afterglow properties would help us to better constrain the physics of GRBs and relativistic jets. Thus many au-

\* D. Turpin used funds provided by the LabEx OCEVU.

thors discussed correlation between the afterglow luminosity and the prompt energetics in the rest frame.

Correlations between the afterglow optical luminosity and prompt isotropic energy have been found by Kann et al. (2010), Nysewander et al. (2009) and also between the afterglow X-ray emission and the isotropic energy by Kaneko et al. (2007) and Margutti et al. (2013). However, it is difficult to assess whether these relations have their origin in the physics of the GRB since some studies have shown that they could undergo strong selection effects. Indeed, recently Coward et al. (2014) detected a strong Malmquist bias in the correlation  $E_{iso} - L_{opt,X}$  as we preferentially detect the brightest part of the GRB population. Other studies lead by Heussaff et al. (2013) and Shahmoradi (2013) have shown that gamma-ray selection effects strongly biased rest frame prompt properties correlations and particularly the  $E_{pi} - E_{iso}$  relation discovered by Amati et al. (2002). While it is clear that gamma-ray selection effects can bias statistical studies of prompt GRB properties, the impact of optical selection effects is rarely assessed. This paper is dedicated to the study of the impact of afterglow optical brightness on the  $E_{pi} - E_{iso}$  relation which is one of the most robust and tightest rest frame prompt correlation. To check the impact of optical selection effects, we construct a sample of GRBs with good optical and gamma-ray data in section 2. In section 3 we describe the optical brightness distribution of GRB in our sample and the potential parameters (extrinsic and intrinsic) that could bias it. Then, we compare the optical brightness of GRBs located at different positions in the  $E_{pi} - E_{iso}$  plane in section 4. In section 5, we briefly discuss the consequences of our findings. Our conclusions are given in section 6.

## 2. GRB sample and data

### 2.1. Optical data

We collected the afterglow optical lightcurves of 126 GRBs with a redshift and 42 GRBs without a redshift. We specifically choose the R band because it concentrates the largest number of optical measurements. These R band photometric measurements are issued from published articles and GCN Circulars<sup>1</sup>.

Then, we used the apparent R magnitude measured 2 hours after the burst without any extinction correction as a proxy for the observed brightness of the optical afterglow. The R magnitude is directly interpolated from the available measurements. To do so, we required that GRBs in our sample have good optical follow up during the first hours after the burst to accurately measure the optical flux of the afterglow. The afterglow light curves of our complete sample of GRBs can be seen in figure 1.

The choice of the time (2 hours after the trigger) at which we measure the optical brightness results from various constraints:

- We want the afterglow to be in its classical slow cooling and decaying regime, yet to be bright enough to permit reliable measurements of the magnitude. However, we removed few GRBs, like GRB060206 (Woźniak et al. 2006; Monfardini et al. 2006), which exhibit strong optical flaring at that time.
- Above all, we want to measure the optical brightness at a time comparable with the time at which the vast majority of GRB redshifts are measured *i.e.* in the first few hours after the trigger.

We also decided to exclude few GRBs with high visual extinction such that  $A_V^{tot} = A_V^{Gal} + A_V^{Host} > 1.2$ . Indeed, GRB afterglows which are strongly absorbed by dust do not bring any

information on their true optical brightness. This cut off is a good trade-off to optimize the number of GRBs for which afterglow brightness isn't so much polluted by strong external effects (dust absorption). The galactic extinction  $A_V^{Gal}$  has been calculated from the dust map of Schlegel et al. (1998) and the host extinctions  $A_V^{Host}$  are issued from varying sources. However, for some bursts we didn't have access to the host extinction. In order to have a rough estimate of it we performed a simple linear fit between  $A_V^{Host}$  and the intrinsic X-ray absorption  $NH_{X,i}$  derived from the Swift XRT catalogue<sup>2</sup>. For this fit we had 114 GRBs available. The best fit gives us the following relation :  $A_V^{Host} = 3.9 \times 10^{-23} \times NH_{X,i} + 0.06$  with a standard deviation of  $\sigma \sim 0.34$  magnitude that we considered as an acceptable uncertainty in our  $A_V^H$  estimates.

At last, for GRB afterglows with only upper limit of detection, we required that their optical upper limit are deeply constrained by large telescopes (at least one 2.0 meter telescope). Moreover, to be selected these upper limits of detection must have been measured close to 2 hours after the burst.

After passing the optical selection criteria we finally ended with 71 GRBs with a redshift (69 detections and 2 upper limits) and 14 GRBs without one (3 detections and 11 upper limits). These 85 GRBs constitute our full sample which is summarized in Table 5 for GRBs with a redshift and Table 6 for GRBs without a redshift. This sample covers about 15 years of pre-Swift and Swift GRB observations (from 1999 to 2014).

### 2.2. Gamma-ray data

For our selected GRBs we also collected the observed gamma-ray properties of the prompt emission : the spectral indexes  $\alpha$  and  $\beta$ , the time for which 90% of the energy is released,  $T_{90}$ , the gamma-ray fluence  $S_\gamma$  and the observed peak energy of the spectral energy distribution  $E_{po}$ . Our gamma-ray selection criteria followed a similar procedure as Heussaff et al. (2013). We selected events with well measured spectral parameters from the GCN Circulars & (Pélangéon et al. 2008; Gruber et al. 2014). We parametrize GRB spectra with the Band function, Band et al. (1993), that consists of two smoothly connected power laws. Following standard naming, we call  $\alpha$  the photon spectral index of the low-energy power law ( $\alpha > -2$ ), and  $\beta$  the photon spectral index of the high-energy power law ( $\beta < -2$ ). The  $\nu F_\nu$  spectrum peaks at the energy  $E_{po}$ , near the junction of the two power laws. The selection was made with the application of the following cuts:

- First, we made a selection on the duration. We considered GRBs with  $T_{90}$  between 2 and 1000 s. This criterion excludes short GRBs ( $T_{90} < 2s$ ), and very long GRBs that are superimposed on a varying background and whose  $E_{peak}$  is difficult to measure accurately.
- Second, we require accurate spectral parameters. We excluded GRBs with one or more spectral parameters missing. We excluded GRBs with an error on alpha (the low-energy index of the Band function) larger than 0.5. We excluded a few GRBs with  $\alpha < -2.0$  and GRBs with  $\beta > \alpha$  because such values suggest a confusion between fitting parameters. We excluded GRBs with large errors on  $E_{po}$ , defined by a ratio of the 90% upper limit to the 90% lower limit larger than 3.5. We have less stringent constraints on beta (the high-energy index of the Band function) since we have checked that the position of GRBs in the  $E_{pi} - E_{iso}$  plane changes very little

<sup>1</sup> <http://gcn.gsfc.nasa.gov>

<sup>2</sup> [http://www.swift.ac.uk/xrt\\_live\\_cat/](http://www.swift.ac.uk/xrt_live_cat/)

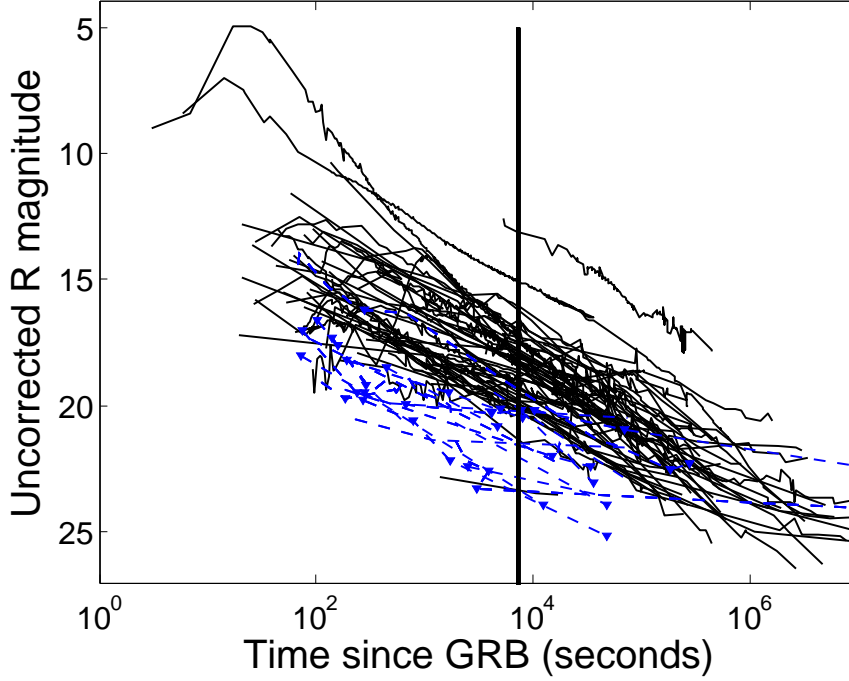


**Fig. 1.** R band optical lightcurves in the observer frame of the afterglows of 71 GRBs with a redshift (black solid line) and 14 GRBs without a redshift (blue dashed line with triangle for upper limits) considered in this study. The magnitudes are not corrected from the galactic and host extinctions. The vertical solid line represents the time (2 hours) at which we estimate the uncorrected R magnitude.

with beta. When the error on  $\beta$  in the catalog is lacking or larger than 1.0, we assigned to  $\beta$  the classical value of 2.3 and we give no error. In a few cases, the high energy spectral index in the Fermi catalog is incompatible with being  $\gamma < 2.0$  at  $2\sigma$  level, and the catalog gives the energy of a spectral break that is not  $E_{po}$ . In these cases we look for  $E_{po}$  in the GCN Circulars, and if we cannot find it, we simply remove the burst from the sample.

### 3. Afterglow optical brightness and intrinsic luminosity

The afterglows of our 85 GRBs span a large range of optical brightness from  $\text{mag } R^{2h} = 13.02$  to  $\text{mag } R^{2h} = 23.9$ , see figure 2. We noticed that GRBs without a redshift have faint optical counterparts which can't be due to high visual extinction since they pass our optical selection criteria. These GRBs are probably high- $z$  GRBs or they could have intrinsically sub-luminous afterglows. Our GRBs with a redshift are also distributed in a wide range of redshift from  $z=0.168$  to  $z=8.26$  and we need to understand if the distribution of the R magnitudes is dominated by the redshift distribution of our GRBs. To verify this hypothesis we separate our 71 GRBs with a redshift into three classes of afterglow brightness equally populated.

1. The class of *bright* GRBs is composed of 24 GRBs with afterglow optical brightness brighter than  $R=17.9$

2. The class of *intermediate brightness* GRBs is composed of 23 GRBs with afterglow optical brightness in the range  $17.9 < R \leq 19.1$
3. The class of *faint* GRBs is composed of 24 GRBs with afterglow optical brightness fainter than  $R=19.1$

We will refer to these classes all along this paper.

#### 3.1. Impact of the redshift on the afterglow optical brightness distribution

We find that The median redshift for the three classes of GRBs are  $z_{med}^{bright} = 1.38$ ,  $z_{med}^{int} = 1.52$  and  $z_{med}^{faint} = 1.87$ . We then compare the redshift distribution of the three classes of GRBs with a Kolomogorov-Smirnov statistical test (KS test). The KS test clearly reveals that the redshift distribution of the three classes are similar. The p-value<sup>3</sup> of each test are 0.656 between bright and intermediate GRBs, 0.387 between bright and faint GRBs and 0.711 between intermediate and faint GRBs. This indicates that the redshift should not bias the optical brightness distribution, see figure 3. We perform an additional simple test that consists in bootstrapping  $n$ -times the redshifts between the bright and faint GRBs and calculating the median redshift difference  $\Delta z_{med}$  distribution. Then the probability of obtaining an absolute differ-

<sup>3</sup> The probability of observing a test statistic as extreme as, or more extreme than, the observed value under the null hypothesis

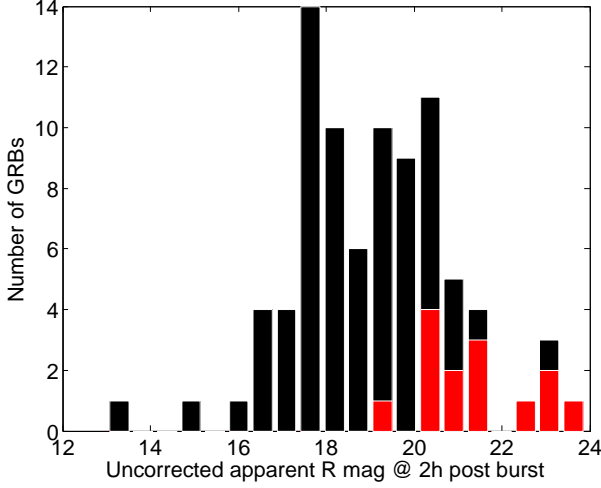


**Fig. 2.** Distribution of the afterglow optical brightness taken 2 hours after the burst (uncorrected R magnitude). The 71 GRBs with a redshift are shown in black and the 14 GRBs without a redshift are in red.

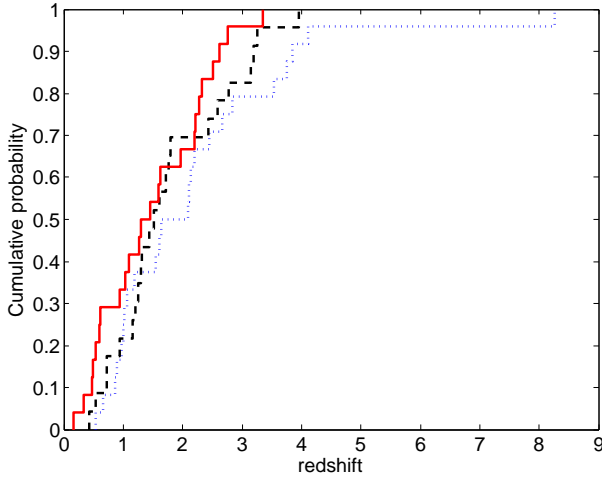


**Fig. 3.** Redshift Cumulative distribution function for our three classes of GRB. The bright, intermediate and faint GRB afterglows are indicated with the solid red, dashed black and dotted blue lines, respectively.

ence  $|\Delta z_{med}|$  at least as strong as we observed with  $N_{tot}$  random simulations is given by :

$$P(X > |\Delta z_{obs}|) = \frac{N(X > |\Delta z_{obs}|)}{N_{tot}}, \text{ here } N_{tot} = 10^5 \quad (1)$$

According to this bootstrapping test, such a redshift difference between bright and faint afterglows is insignificant. This result confirms that the redshift doesn't drive the observed optical flux. The results of the statistical tests are summed up in table 1.

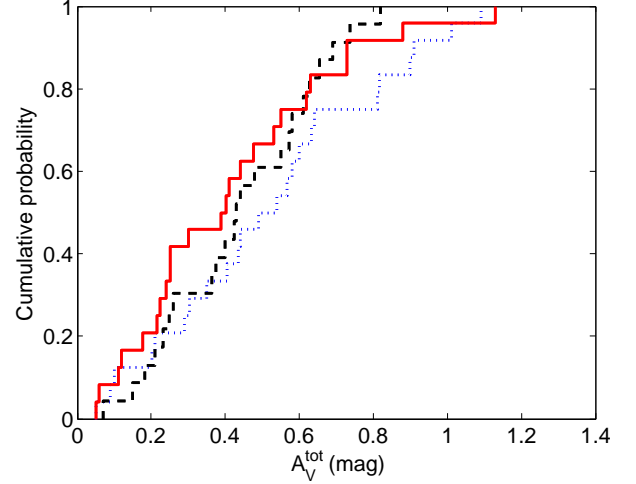


**Fig. 4.** Cumulative distribution function of  $A_V^{tot}$  for our three classes of GRB. The bright, intermediate and faint GRB afterglows are indicated with the solid red, dashed black and dotted blue lines, respectively.

### 3.2. Impact of the visual extinction in the afterglow optical brightness distribution

Albeit we have selected GRBs with relatively low total visual extinction ( $A_V^{tot} < 1.2$ ) we also checked if this parameter could bias our afterglow brightness distribution, i.e. whether faint afterglows are more obscured by dust. We found  $median[A_V^{tot}_{bright}] = 0.39$  for bright GRBs,  $median[A_V^{tot}_{int}] = 0.43$  for intermediate GRBs and  $median[A_V^{tot}_{faint}] = 0.54$  for faint GRBs. We performed a KS-test to compare the  $A_V^{tot}$  distribution of our three classes of GRB afterglow brightness, see figure 4. We found that the three populations of GRBs are drawn from the same underlying distribution. For example, a p-value as high as 0.622 is found between bright and faint GRBs. We also performed a bootstrapping test to compare the total visual extinction of bright and faint GRB afterglows. This test is completely compatible with the result of the KS test, see table 1 for the complete results of our statistical tests. We conclude that our selected GRBs with faint afterglows are as obscured as the bright ones and thus visual extinction doesn't drive our afterglow optical distribution.

### 3.3. Afterglow intrinsic optical luminosity

As the extrinsic factors (redshift, visual extinction) don't seem to play a major role in the observed optical brightness distribution, we investigated the impact of the intrinsic optical luminosity of the afterglows. We calculated the optical luminosity density (in units of erg/s/Hz) taken two hours *in the rest frame* using the formula:

$$L_R(t_{rest}) = \frac{4\pi D_L(z)^2}{(1+z)^{1-\beta_o+\alpha_o}} \times F_R(t_{obs}) \left( \frac{\nu_R}{\nu_{obs}} \right)^{-\beta_o} \quad (2)$$

where  $F_R$  is the optical flux density corrected from the Galactic and host extinction measured at  $t_{obs} = 2h$  after the burst in the observer frame,  $z$  is the GRB redshift,  $D_L(z)$  is the luminosity distance,  $\beta_o$  is the optical spectral index and  $\alpha_o$  is

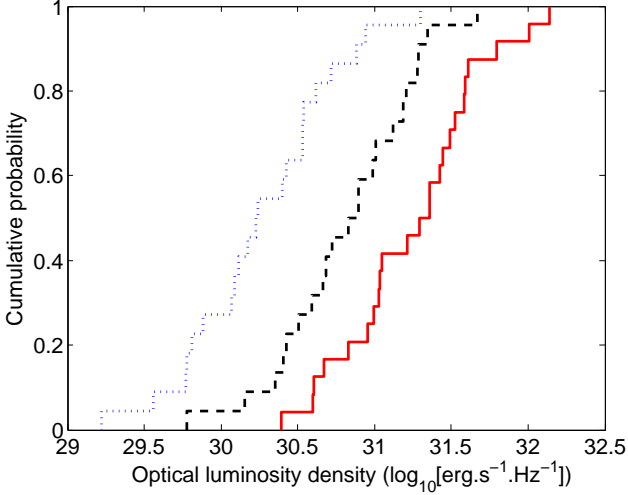


**Fig. 5.** Cumulative distribution function of the optical luminosity density (taken 2h after the burst in the rest frame) for our three classes of GRB. The bright, intermediate and faint GRB afterglows are indicated by the solid red, dashed black and dotted blue lines, respectively.

the optical temporal index,  $\nu_R$  is the typical frequency of the R band (Vega system) and  $\nu_{obs}$  is the observed frequency (here  $\nu_{obs} = \nu_R$ ). For GRBs with no optical detection we used their optical upper limits to compute the  $F_R$  and the value of  $\alpha_o^{med}$  and  $\beta_o^{med}$  to estimate an upper limit on their optical luminosity density.

Then, we compared the optical luminosity densities in the rest frame of the three classes of GRB brightness (*bright*, *intermediate* and *faint*), see figure 5. To do so, we apply the same statistical tests than previously. The KS test reveals that :

- the population of bright and faint GRBs have very different optical luminosity density distribution with a p-value of  $1.73 \times 10^{-6}$  ( $\sim 5\sigma$  confidence level).
- the population of bright and intermediate GRBs have marginally different optical luminosity density distribution with a p-value of  $1.126 \times 10^{-2}$  ( $\sim 2.5\sigma$  confidence level).
- the population of intermediate and faint GRBs have different optical luminosity density distribution with a p-value of  $4.861 \times 10^{-3}$  ( $\sim 3\sigma$  confidence level).

The median optical luminosity densities (in log scale) for the three classes of GRBs are  $LR_{med}^{bright} = 31.33 \text{ erg.s}^{-1}.\text{Hz}^{-1}$ ,  $LR_{med}^{int} = 30.86 \text{ erg.s}^{-1}.\text{Hz}^{-1}$  and  $LR_{med}^{faint} = 30.23 \text{ erg.s}^{-1}.\text{Hz}^{-1}$ . We observe that faint GRBs are one order of magnitude less luminous on average than bright GRBs ( $\Delta L_R = 1.1 \text{ erg.s}^{-1}.\text{Hz}^{-1}$ ). The bootstrapping simulations of the optical luminosity density between the class of bright and faint GRBs show that such observed  $\Delta L_R$  is never seen in the total random cases ( $10^5$  simulations) making this difference of luminosity highly significant. The results of the statistical tests are summed up in table 1. We conclude that our afterglow optical brightness distribution is strongly shaped by the intrinsic optical luminosity densities of the GRB afterglows. Moreover, the GRBs without a redshift also follow this trend. Indeed, they have faint afterglows in the observer frame (see figure 2) and at any redshift,

most of them would have had intrinsically under luminous afterglows, see figure 6. Thus, we conclude that a large population of GRBs with intrinsic faint afterglows may escape detection in the optical domain creating a strong bias in the afterglow intrinsic luminosity distribution. We particularly remarked that GRBs with  $L_R < 30.0 \log_{10}(\text{erg.s}^{-1}.\text{Hz}^{-1})$  are systematically not beyond  $z \sim 1$ , except for GRB090519.

### 3.4. The case of GRB 090519

GRB 090519 is one exception of a very faint GRB with a redshift measurement that illustrates the optical selection effects that a large population of GRBs undergo. GRB090519 was both detected by Fermi and Swift on 2009 May 19 at 21:08:56 UT, see Perri et al. (2009). Swift-XRT and Swift-UVOT rapidly observed the field of GRB090519 (130s after the burst). An X-ray counterpart was clearly identified by Swift-XRT allowing a refined localization of the burst at  $\text{RA}(J2000) = 09^h29^m06.85^s$  and  $\text{Dec}(J2000) = +00^\circ10'48.6''$ . However, no significant optical counterpart was detected by Swift-UVOT and a corresponding 3-sigma upper limit of 19.6 mag (white filter) was estimated at  $\sim 200$ s after the burst. On the ground, fast robotic telescopes rapidly respond to the GCN notice as TAROT at Calern observatory in France, Klotz et al. (2009a), FARO at Chante Perdrix Observatory in France, Klotz & Kugel (2009), and BOOTES-1B in Spain Jelinek & Kubanek (2009). No optical counterpart was detected and a limiting magnitude of  $R_i 18.5$  at  $t \sim 230$ s after the burst was estimated from TAROT Calern observations. The low galactic extinction ( $A_V^{gal} = 0.13$ ) suggested that GRB090519 is a high- $z$  GRB or is embedded in a very dusty environment. In the next hours, NOT, see Thoene et al. (2009c), and GROND telescope, see Rossi et al. (2009b), detected a new fading optical source in the XRT field of view which was associated to the afterglow emission from GRB090519. The magnitude measured by NOT at  $t \sim 0.33$ h after the burst was  $R \sim 22.8$  revealing that the afterglow of GRB090519 is among the faintest afterglow ever observed, see figure 1. The faintness of the afterglow was due to a combination of a high redshift value and an intrinsic weak luminosity of the afterglow, see figure 6. We estimate from its high  $NH_{X,i}$  measurement a high  $A_V^{Host} = 0.96$ , however Greiner et al. (2011) found  $AV_{Host} \sim 0.01$  by fitting GROND/Swift-XRT broadband spectrum. So, we exclude a very dusty environment surrounding GRB 090519 and this burst should be even intrinsically fainter than the value we report here with a  $A_V^{Host} = 0.96$ . Albeit faint, the redshift of GRB090519 was determined by the VLT, see Thoene et al. (2009b), thanks to a fast response to the GCN notice ( $\sim 4$  h after the burst). We can reasonably believe that a delay of a few additional hours in the VLT observation schedule would have made the afterglow of GRB090519 unreachable for a redshift measurement and useless for GRBs studies.

## 4. Optical selection effect in the $E_{pi} - E_{iso}$ plane

With the first measurement of a GRB redshift in 1997, came the possibility to measure the intrinsic properties of GRBs. Few years later, Amati et al. (2002) discovered a strong correlation linking the energy of the maximum of the prompt emission,  $E_{pi}$ , and  $E_{iso}$ , the isotropic energy of GRBs. Since  $E_{iso}$  depends on the cosmology, and  $E_{pi}$  is cosmology free, this relation has been used by various authors to standardize GRBs, and eventually to constrain the parameters of cosmological models (e.g. Schaefer & Collazzi 2007; Amati & Valle 2013). It was also used as a tool to infer GRB redshifts (Atteia 2003; Xiao & Schaefer

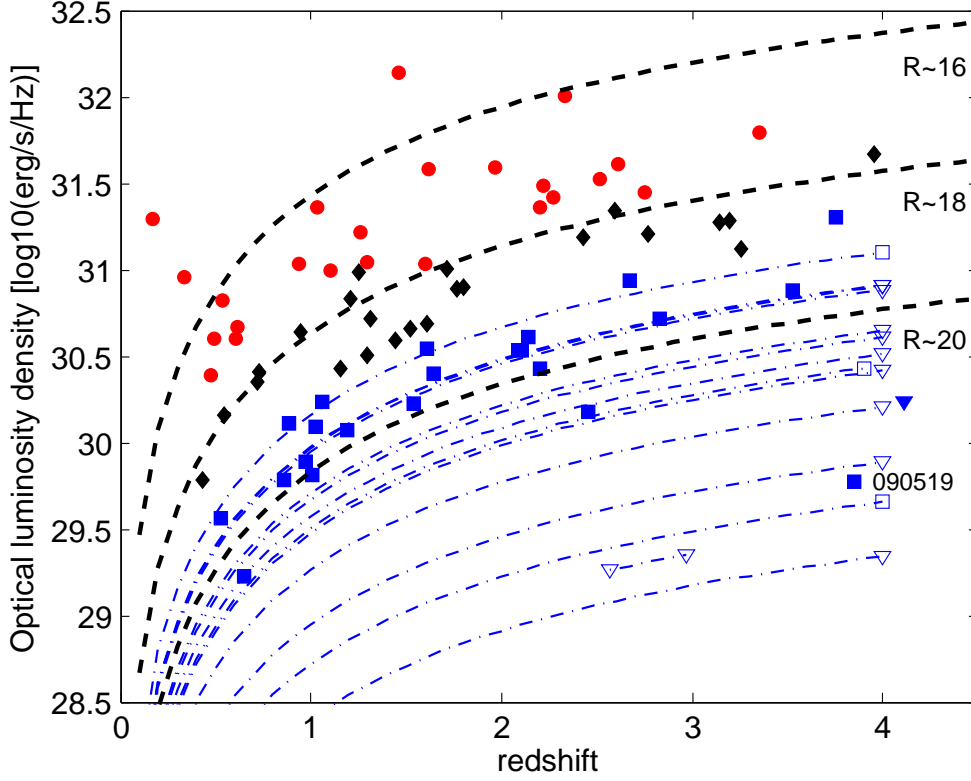


**Fig. 6.** Intrinsic optical luminosity density as a function of redshift for 71 GRBs with a redshift and 14 GRBs without a redshift (blue dash-dotted lines). Upper limit are plotted as downward triangles. The red circles represent bright GRBs in the observer frame, the black diamonds represent intermediate GRBs in the observer frame and faint GRBs in the observer frame are plotted as blue squares.

2009), to constrain the physics of the prompt emission (Eichler & Levinson 2004; Rees & Mészáros 2005) and the geometry of GRB jets (Lamb et al. 2005; Toma et al. 2005). However, few years after this discovery, other studies showed that this relation could be affected by various selection effects, raising a debate about the reality of the  $E_{\text{pi}} - E_{\text{iso}}$  relation (e.g. Band & Preece 2005; Ghirlanda et al. 2005; Nakar & Piran 2005; Sakamoto et al. 2006; Butler et al. 2007; Cabrera et al. 2007; Schaefer & Collazzi 2007; Butler et al. 2009; Firmani et al. 2009; Krimm et al. 2009; Butler et al. 2010; Shahmoradi & Nemiroff 2011; Collazzi et al. 2012; Kocevski 2012; Goldstein 2012). Heussaff et al. (2013) proposed to explain these conflicting results with the combination of two effects: a true lack of GRBs with large  $E_{\text{iso}}$  and low  $E_{\text{pi}}$  and selection effects preventing the detection of GRBs with low  $E_{\text{iso}}$  and large  $E_{\text{pi}}$ , which have comparatively less photons. While they mainly investigated the selection effects related with the detection of the prompt gamma-ray photons, Heussaff et al. (2013) also mentioned the possible impact of optical selection effects on the  $E_{\text{pi}} - E_{\text{iso}}$  relation, without investigating this possibility in detail. This issue is discussed in this section.

#### 4.1. Our GRB sample in the $E_{\text{pi}} - E_{\text{iso}}$ plane

Our selected 71 GRBs with a redshift follow a standard  $E_{\text{pi}} - E_{\text{iso}}$  relation, as shown in figure 7. The best fit  $E_{\text{pi}} - E_{\text{iso}}$  relation for this sample is  $E_{\text{pi}} = 126 E_{52}^{0.504}$  keV, where  $E_{52}$  is the GRB isotropic energy in units of  $10^{52}$  ergs (see figure 7). This best fit relation is fully compatible with the  $E_{\text{pi}} - E_{\text{iso}}$  relation found by other authors (e.g. Nava et al. 2012; Gruber et al. 2012), showing that our sample is not significantly biased for what concerns the distribution of GRBs with a redshift in the  $E_{\text{pi}} - E_{\text{iso}}$  plane. The dispersion of the points around the best fit relation along the vertical axis,  $\sigma = 0.29$ , is also comparable with the values found by Nava et al. (2012) and Gruber et al. (2012), ( $\sigma = 0.34$ ).

#### 4.2. Afterglow optical brightness in the $E_{\text{pi}} - E_{\text{iso}}$ plane

In order to investigate the distribution of the afterglow optical brightnesses in the  $E_{\text{pi}} - E_{\text{iso}}$  plane, we did two complementary analysis. One comparing the vertical distance to the best fit  $E_{\text{pi}} - E_{\text{iso}}$  relation for the three classes of GRB afterglow brightness and a second comparing the afterglow optical brightness of GRBs located above and below the best fit  $E_{\text{pi}} - E_{\text{iso}}$  relation.



**Table 1.** Result of the different statistical tests (Kolomogorov-Smirnov, bootstrap). The probabilities indicated correspond to the p-values, i.e, the probability of observing a test statistic as extreme as, or more extreme than, the observed value under the null hypothesis

Median value	Tested parameter	KS test (p-value)	Bootstrap test (p-value)
$z^{bright} = 1.38$	$\Delta z_{int}^{bright}$	0.66	0.73
$z^{int} = 1.52$	$\Delta z_{faint}^{bright}$	0.38	0.34
$z^{faint} = 1.87$	$\Delta z_{faint}^{int}$	0.71	0.31
$A_V^{bright} = 0.39$	$\Delta A_V^{bright}_{int}$	0.92	0.56
$A_V^{int} = 0.43$	$\Delta A_V^{bright}_{faint}$	0.62	0.24
$A_V^{faint} = 0.54$	$\Delta A_V^{int}_{faint}$	0.65	0.47
$L_R^{bright} = 31.33 \text{ erg.s}^{-1}.\text{Hz}^{-1}$	$\Delta L_R^{bright}_{int}$	$1.26 \times 10^{-2}$	0.005
$L_R^{int} = 30.86 \text{ erg.s}^{-1}.\text{Hz}^{-1}$	$\Delta L_R^{bright}_{faint}$	$1.73 \times 10^{-6}$	$< 10^{-5}$
$L_R^{faint} = 30.23 \text{ erg.s}^{-1}.\text{Hz}^{-1}$	$\Delta L_R^{int}_{faint}$	0.005	$2.3 \times 10^{-4}$

#### 4.2.1. Comparing the vertical distances

The vertical distance is defined as  $\log_{10}(E_{pi}) - \log_{10}[\text{bestfit}(E_{pi} - E_{iso} \text{ relation})]$  and we show in figure 8 our GRB sample in a plane combining the vertical distances to the best fit  $E_{pi} - E_{iso}$  relation and the afterglow optical brightness. We found that the median vertical distance of the bright GRBs is  $dist_{med}^{bright} = -0.07$ ,  $dist_{med}^{int} = -0.09$  for the intermediate GRBs and  $dist_{med}^{faint} = 0.16$  for the faint GRBs. We performed a KS test to compare the vertical distance distributions for our three class of GRBs. The KS test reveals that the two populations of bright and faint GRBs are drawn from two different underlying distributions with a p-value  $= 9.31 \times 10^{-4}$ , see figure 9. We also calculated the KS-test between the bright and intermediate GRBs and between the intermediate and faint GRBs. These tests reveal that intermediate and bright GRBs obey to the same distribution while faint GRBs clearly differ from the two other group of GRBs. To verify the validity of the KS-test we perform a bootstrapping simulation considering the vertical distances and we also find that faint GRBs differ from the other group of GRBs. The results of statistical tests are summed up in table 2.

These two statistical tests confirm that GRBs with faint afterglows are preferentially located above the best fit  $E_{pi} - E_{iso}$  relation (18/24 faint GRBs are "above") whereas bright GRBs are generally located below the best fit  $E_{pi} - E_{iso}$  relation (17/24 bright GRBs are "below"). This particular distribution of the afterglow optical brightnesses in the  $E_{pi} - E_{iso}$  plane is significant at the level  $3\sigma$ .

#### 4.2.2. Comparing the afterglow optical brightness with respect to the best fit $E_{pi} - E_{iso}$ relation

We performed a complementary analysis, looking if we can find a significant difference in optical brightness between GRBs lo-

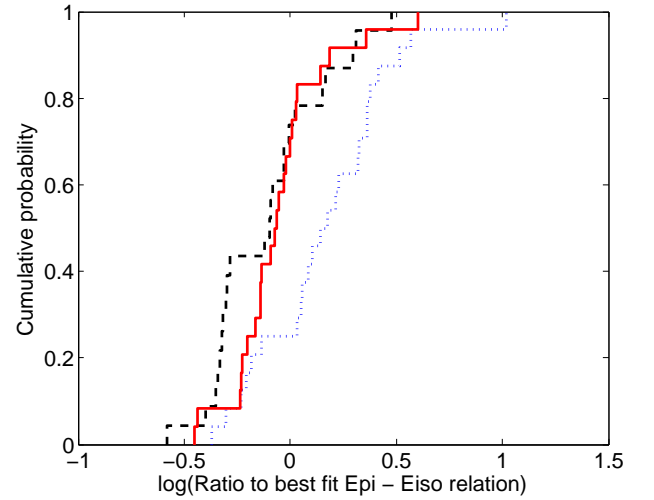


**Fig. 9.** Cumulative distribution function of the vertical distance to the best fit  $E_{pi} - E_{iso}$  relation for our three classes of GRB. The bright, intermediate and faint GRB afterglows are indicated with the solid red, dashed black and dotted blue lines, respectively.

cated above and below the best fit  $E_{pi} - E_{iso}$  relation, see figure 8. We compared the optical brightness (R magnitude) of the two groups of GRBs. In order to include GRBs without a redshift, we calculated their minimum and maximum vertical distance to the best fit  $E_{pi} - E_{iso}$  relation. Then we only kept those which are strictly above the best fit  $E_{pi} - E_{iso}$  relation or strictly below it at all redshifts considered here ( $0.34 < z < 3.72$ ). 7 GRBs without a redshift were selected and all of them were strictly located

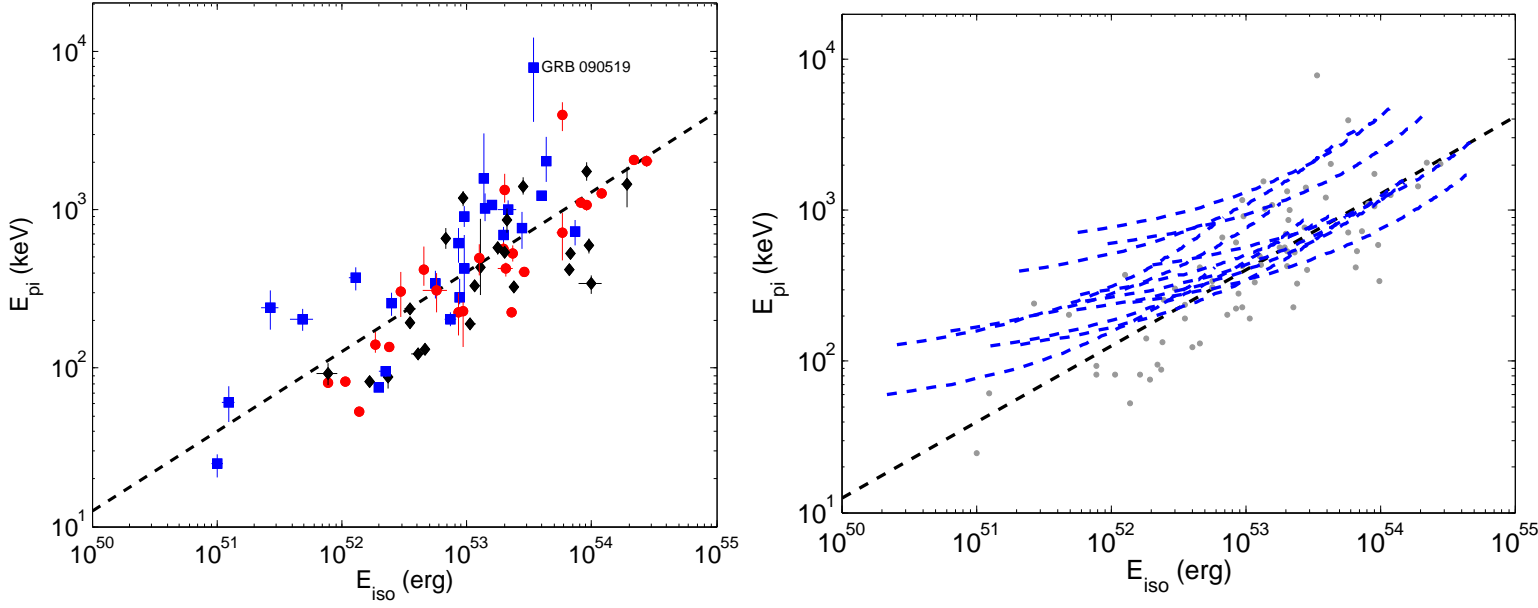


**Fig. 7.** Distribution of the 71 GRBs with a redshift (left panel) and the 14 GRBs without a redshift (right panel) in the  $E_{\text{pi}} - E_{\text{iso}}$  plane. Left panel : The red circles corresponds to the population of GRBs with bright afterglows, the black diamonds corresponds to the GRB with intermediate brightness and the blue squares corresponds to the faint GRB afterglows. Right panel : The dashed lines represents the possible location of the GRBs without a redshift in the  $E_{\text{pi}} - E_{\text{iso}}$  plane and their color shows their class of afterglow brightness (red = bright, black = intermediate, blue = faint). The grey dots indicate the location of our 71 GRBs with a redshift in the  $E_{\text{pi}} - E_{\text{iso}}$  plane. Both panels : The best fit  $E_{\text{pi}} - E_{\text{iso}}$  relation is represented as the black dashed solid line, which is fully compatible with other recent studies (e.g. Nava et al. 2012; Gruber et al. 2012).

above the best fit  $E_{\text{pi}} - E_{\text{iso}}$  relation. So, we finally used 78 GRBs in the analysis.

First, we compared the afterglow optical brightness distribution of GRBs above and below the best fit  $E_{\text{pi}} - E_{\text{iso}}$  relation applying a KS-test. The statistical test confirms that the two distributions clearly differ with a p-value  $p = 1.41 \times 10^{-5}$ . We found that the mean R magnitude of the GRBs located above the best fit  $E_{\text{pi}} - E_{\text{iso}}$  relation (38 GRBs) is  $R_{\text{mean}}^{\text{above}} = 19.69$ , while the GRBs below the best fit  $E_{\text{pi}} - E_{\text{iso}}$  relation (40 GRBs) have  $R_{\text{mean}}^{\text{below}} = 18.1$ . We again performed bootstrapping simulations (with the R magnitudes) to evaluate the significance of such brightness difference ( $\Delta R_{\text{mean}} = 1.59$ ) between GRBs "above & below". An R magnitude difference as strong as we observe is obtained in only 0.003% of the cases, indicating that it is significant at the level of 99.997% ( $> 4\sigma$  confidence level), see figure 10. The high significance of these tests confirm that GRBs located below the best fit  $E_{\text{pi}} - E_{\text{iso}}$  relation have brighter afterglows than those of GRBs located above it. The results of the statistical tests are summed up in table 2.

#### 4.3. Consequence for the $E_{\text{pi}} - E_{\text{iso}}$ relation and other GRB correlations

According to these results, we conclude that there is a significant correlation between the afterglow optical brightness of our GRB sample and their location in the  $E_{\text{pi}} - E_{\text{iso}}$  plane. Faint GRBs preferentially fill in the region above the best fit  $E_{\text{pi}} - E_{\text{iso}}$  relation and conversely for the bright GRBs which fill preferentially the region below the best fit  $E_{\text{pi}} - E_{\text{iso}}$  relation. This effect could

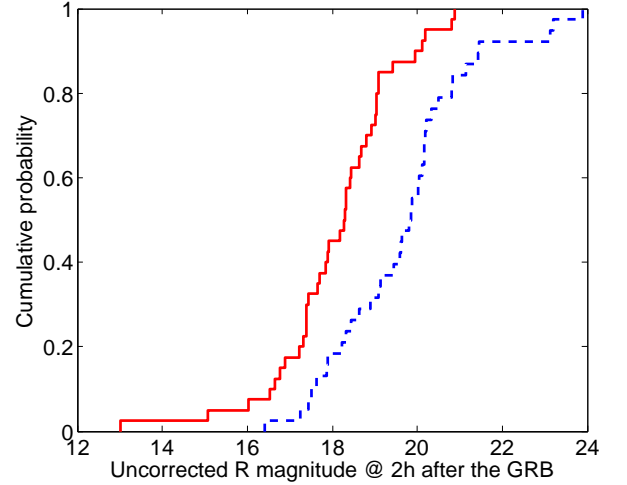


**Fig. 10.** Cumulative distribution function of the afterglow R magnitudes. The 38 GRBs located above the best fit  $E_{\text{pi}} - E_{\text{iso}}$  relation are indicated with the blue dashed line while the 40 GRBs located below the best fit  $E_{\text{pi}} - E_{\text{iso}}$  relation are represented with the red solid line.

prevent many GRBs in the upper part of the  $E_{\text{pi}} - E_{\text{iso}}$  plane from having a redshift measurement. Indeed, we noticed that the



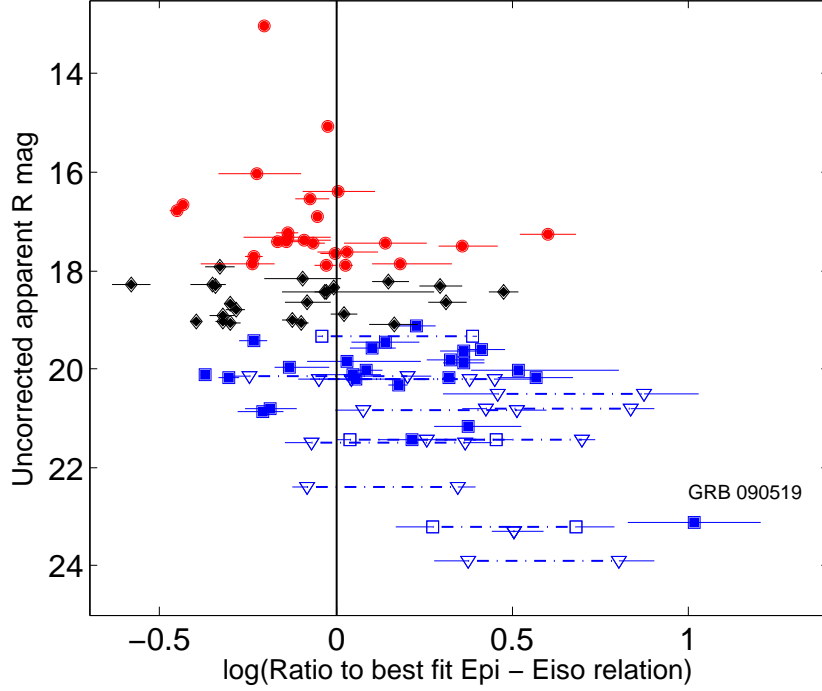


**Fig. 8.** Distribution of the afterglow optical brightness as a function of their vertical distance to the  $E_{\text{pi}} - E_{\text{iso}}$  relation. The black solid line separates the population of GRBs located above ( $\text{dist} > 0$ ) and below ( $\text{dist} < 0$ ) the best fit  $E_{\text{pi}} - E_{\text{iso}}$  relation. The red circles represent the class of bright GRBs, the black diamonds represent the GRBs of intermediate brightness and the blue squares represent the faint GRBs. The upper limit of detections are plotted as downward triangles. The GRBs without a redshift are represented with dash dotted line showing their maximum and minimum vertical distance to the  $E_{\text{pi}} - E_{\text{iso}}$  relation.

**Table 2.** Result of the different statistical tests (Kolmogorov-Smirnov, bootstrap). The probabilities indicated correspond to the p-values, i.e, the probability of observing a test statistic as extreme as, or more extreme than, the observed value under the null hypothesis

Median value	Tested parameter	KS test (p-value)	Bootstrap test (p-value)
$\text{dist}^{\text{bright}} = -0.07$	$\Delta \text{dist}_{\text{int}}^{\text{bright}}$	0.084	0.62
$\text{dist}^{\text{int}} = -0.09$	$\Delta \text{dist}_{\text{faint}}^{\text{bright}}$	$9.31 \times 10^{-4}$	$9.0 \times 10^{-3}$
$\text{dist}^{\text{faint}} = 0.16$	$\Delta \text{dist}_{\text{faint}}^{\text{int}}$	$1.40 \times 10^{-3}$	0.026
$R_{\text{mag}}^{\text{above}} = 19.69$ $R_{\text{mag}}^{\text{below}} = 18.10$	$\Delta R_{\text{mag}}^{\text{above}}$	$1.41 \times 10^{-5}$	$3.0 \times 10^{-5}$

majority of GRBs without a redshift, which have very faint afterglows (fainter than  $R=20$  mag at 2h after the burst) are mainly located in the upper part of the  $E_{\text{pi}} - E_{\text{iso}}$  plane. Thus, we confirm that the  $E_{\text{pi}} - E_{\text{iso}}$  relation is not immune to significant optical selection effects that could jointly act with the gamma-ray selection effect against the detection of a wider population of GRBs in the upper part of the  $E_{\text{pi}} - E_{\text{iso}}$  plane. In addition, as the redshift is a crucial ingredient to study GRB rest frame properties, it's clear

that optical selection effects would also apply to other GRB rest frame correlations.

#### 4.4. Using the $E_{\text{pi}} - E_{\text{iso}}$ relation for cosmology

Despite the existence of significant selection effects in the  $E_{\text{pi}} - E_{\text{iso}}$  plane we observed that GRBs brighter than  $R_{\text{mag}} \sim 19.7$  are rather symmetrically distributed around the best fit  $E_{\text{pi}} - E_{\text{iso}}$  relation. Below that optical brightness, GRBs are clearly concen-

trated towards the upper part of the  $E_{\text{pi}} - E_{\text{iso}}$  plane, see figure 8. First, this means that bright GRBs may indeed follow a standard  $E_{\text{pi}} - E_{\text{iso}}$  relation and could be suitable for cosmological studies based on this correlation. Second, faint and dark GRBs cannot be used for cosmological studies in the same way as bright GRBs, especially since they are not compatible with the  $E_{\text{pi}} - E_{\text{iso}}$  relation. In any case the selection effects due to the measure of the redshift should be taken into account when discussing the  $E_{\text{pi}} - E_{\text{iso}}$  relation as a genuine rest frame prompt property of long GRBs and when attempting to use it for cosmology. Moreover, as shown in the figure 6, GRBs that can be calibrated with supernovae Ia (at redshifts  $z \lesssim 1.5$ ), are not representative of the GRB population at higher redshift (fig. 6). We have shown in section 3.3 that high- $z$  GRBs are mostly optically intrinsically bright and that a large population of faint GRBs remains undetected, while these faint GRBs represent a significant fraction of the population detected at lower redshifts. According to this feature, we think that cosmological studies using high- $z$  GRBs may undergo large uncertainties.

## 5. Discussion

### 5.1. Impact of the $E_{\text{iso}}$ on the observed afterglow brightness

In the framework of the fireball model, the intensity of the afterglow emission is partly determined by the internal kinetic energy of the jet  $E_k^{52} = E_{\text{iso}}^{52} \times \frac{1-\eta}{\eta}$  where  $\eta$  is the gamma-ray radiative efficiency. Thus, the  $E_{\text{iso}}$  is an important parameter to power optical GRB afterglows. We decided to check if the  $E_{\text{iso}}$  distribution is biased by the optical brightness distribution of GRB's afterglow. First, we calculated the median  $E_{\text{iso}}$  value  $E_{\text{iso}}^{\text{bright}}_{\text{med}} = 53.3 \log_{10}(\text{erg})$  for the bright GRBs,  $E_{\text{iso}}^{\text{int}}_{\text{med}} = 53.1 \log_{10}(\text{erg})$  for the intermediate GRBs and  $E_{\text{iso}}^{\text{faint}}_{\text{med}} = 52.9 \log_{10}(\text{erg})$  for the faint GRBs. We still applied the same statistical method to compare the  $E_{\text{iso}}$  distribution of our three class of afterglow brightness, see figure 11. The KS test reveals that :

- the population of bright and faint GRBs have similar  $E_{\text{iso}}$  distributions with a the p-value of 0.387.
- the population of bright and intermediate GRBs have similar  $E_{\text{iso}}$  distributions with a the p-value of 0.993.
- the population of intermediate and faint GRBs have similar  $E_{\text{iso}}$  distributions with a the p-value of 0.569.

To compare the  $E_{\text{iso}}$  distribution between the bright and faint GRBs, we also performed a simulation based on bootstrapping. According to these two statistical tests, we conclude that the afterglow optical brightness distribution does not bias the observed  $E_{\text{iso}}$  distribution of the GRBs. The results of the statistical tests are summed up in table 3.

### 5.2. Impact of the $E_{\text{pi}}$ on the observed afterglow brightness

We performed the same statistical test for  $E_{\text{pi}}$ . We calculated the median  $E_{\text{pi}}^{\text{bright}}_{\text{med}} = 420.2 \text{ keV}$  for the bright GRBs,  $E_{\text{pi}}^{\text{int}}_{\text{med}} = 421.0 \text{ keV}$  for the intermediate GRBs and  $E_{\text{pi}}^{\text{faint}}_{\text{med}} = 519.6 \text{ keV}$  for the faint ones. Then we applied a KS test to compare the  $E_{\text{pi}}$  distributions of our three class of GRB's afterglow brightness. This test reveals that the three populations of GRB have clearly the same  $E_{\text{pi}}$  distributions, see figure 12. We noted the lack of significance difference between the bright and the faint afterglows measured with the KS test (p-value = 0.861) indicating that optical afterglow brightness does not strongly bias the

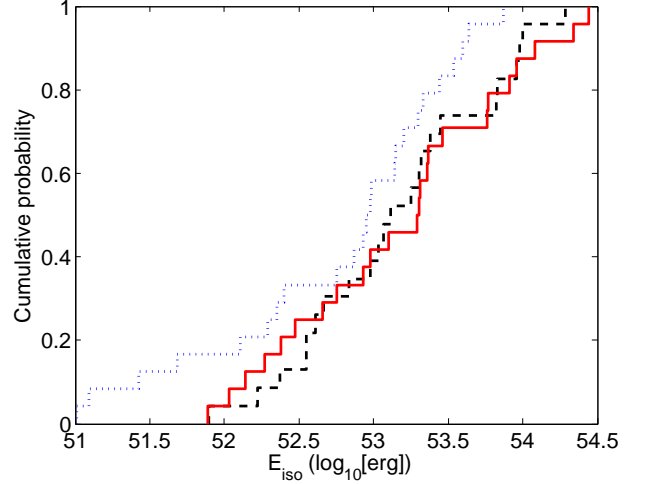


**Fig. 11.** Cumulative distribution function of  $E_{\text{iso}}$  for our three classes of GRBs. The bright, intermediate and faint GRB afterglows are indicated with the solid red, dashed black and dotted blue lines, respectively.

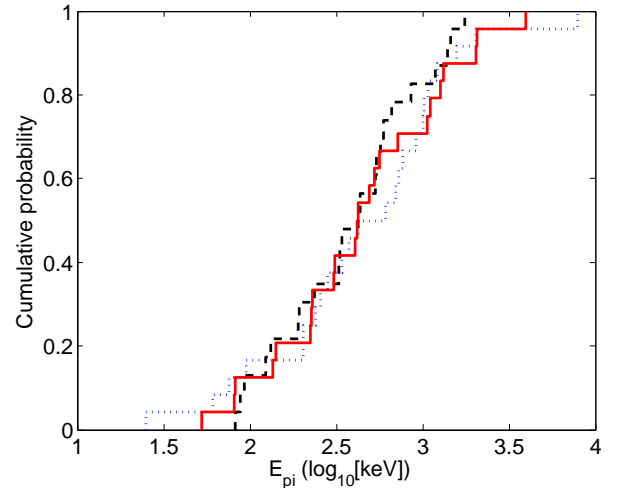


**Fig. 12.** Cumulative distribution function of  $E_{\text{pi}}$  for our three classes of GRBs. The bright, intermediate and faint GRB afterglows are indicated with the solid red, dashed black and dotted blue lines, respectively.

observed  $E_{\text{pi}}$  distribution. As for the previously tested parameter, we performed additional simulations based on bootstrapping the  $E_{\text{pi}}$  between the bright and faint GRBs. We found that a  $E_{\text{pi}}$  difference as we observed ( $\Delta E_{\text{pi}} = 100 \text{ keV}$ ) is not significant. The statistical test results are summarized in table 3.

### 5.3. Redshift measurement

It has been shown by Fynbo et al. (2009) that GRBs with a redshift measured from the spectroscopy of their optical afterglow lack of dark GRBs and have also brighter high energy

**Table 3.** Result of the different statistical tests (Kolomogorov-Smirnov, bootstrap). The probabilities indicated correspond to the p-values, i.e, the probability of observing a test statistic as extreme as, or more extreme than, the observed value under the null hypothesis

Median value	Tested parameter	KS test (p-value)	Bootstrap test (p-value)
$E_{iso}^{bright} = 53.3 \log_{10}(erg)$	$\Delta E_{iso}^{bright}_{int}$	0.99	0.66
$E_{iso}^{int} = 53.1 \log_{10}(erg)$	$\Delta E_{iso}^{bright}_{faint}$	0.39	0.16
$E_{iso}^{faint} = 52.9 \log_{10}(erg)$	$\Delta E_{iso}^{int}_{faint}$	0.57	0.48
$E_{pi}^{bright} = 420 keV$	$\Delta E_{pi}^{bright}_{int}$	0.99	$\sim 1.0$
$E_{pi}^{int} = 421 keV$	$\Delta E_{pi}^{bright}_{faint}$	0.86	0.62
$E_{pi}^{faint} = 520 keV$	$\Delta E_{pi}^{int}_{faint}$	0.45	0.69

emission from the prompt phase than GRBs for which redshift was not determined from the afterglow spectroscopy. These authors also showed that GRBs with a spectroscopic redshift have significantly less X-ray absorption than GRBs with non spectroscopic redshift. They concluded that these GRBs easily detectable are non-representative of the whole GRB population. As GRBs with a spectroscopic redshift represent the majority of the Swift GRBs with a redshift and that the whole population of Swift GRBs is composed of only one third of GRBs with a redshift, this selection effect introduces in GRBs studies (rest frame prompt properties, star forming region of GRBs, standardization of GRBs, etc.) that should not be ignored.

The exceptional case of GRB090519 shows us that it is possible to detect and measure the redshift from faint optical afterglows as soon as large telescopes fastly respond to the GCN notice (few hours after the burst at most) when a very early non detection of an optical counterpart is assessed by fast slewing robotic telescope. It is obvious that a joint observational strategy between fast robotic telescope and very large telescope is needed to measure the redshift of such optically faint GRB population.

A way to reduce this bias from spectroscopic redshift measurement is to look for the host galaxy of GRBs. If it is sufficiently bright and well identified, a redshift can be determined from the spectroscopy of the host galaxy emission line. This work has already been done by Hjorth et al. (2012) with the TOUGH survey realized with the VLT instruments (FORS1, FORS2, ISAAC and X-shooter). They were able to determine 15 new redshifts over 23 host galaxy spectra increasing the redshift completeness of their total sample from 55% to 77%. They also were able to determine with their own TOUGH program 17 redshift larger than  $z=2$ . Such method of redshift measurement should be encouraged in order to enrich the GRB samples and unbiased statistical study of GRBs and host properties.

#### 5.4. The optical afterglow of Fermi GRBs

Our GRB sample is mainly composed of pre-Swift and Swift GRBs and so our study does not take into account the recent GRBs only detected by Fermi-GBM or Fermi-LAT. This could potentially create a bias in our sample since we missed a part

of the GRBs population. However most of Fermi GRBs have no redshift measurements due to the difficulty to locate them with sufficiently high precision. This prevents astronomers from performing optical follow-up with ground based telescopes and spectroscopy of the afterglow optical counterpart. It's clear that this lack of redshift measurements participate to hide numerous Fermi GRBs in the  $E_{pi} - E_{iso}$  plane and so avoid to test the  $E_{pi} - E_{iso}$  relation in the context of Fermi GRBs. Some studies, like (Gruber et al. 2012; Nava et al. 2012; Heussaff et al. 2013) particularly showed that Fermi GRBs with a redshift follow a broader  $E_{pi} - E_{iso}$  relation than pre-Fermi GRBs. Moreover, some outliers (12% of the Fermi GRBs) have been identified by Heussaff et al. (2013). A need for the redshift measurement of Fermi GRBs would be important for GRB studies.

Recently, Singer et al. (2015) reported the results of their intermediate Palomar Transient Factory observational program. This program consists in searching the optical counterparts of Fermi GRBs to perform broadband follow up and spectroscopy (from X-ray to radio). They present broadband observations of 8 Fermi GRBs for which they could derive spectroscopic redshift. We note that they found a new outlier (140606B/PTF14bfu) to the  $E_{pi} - E_{iso}$  relation located at  $z=0.384$ . This kind of study is interesting to test our correlation between the afterglow optical brightness and the GRBs location in the  $E_{pi} - E_{iso}$  plane in the context of Fermi GRBs. According to their optical and gamma-ray data, we have included 6/8 of their GRBs to our analysis (see figure 13) and found that they confirm it, slightly improving the significance of the magnitude difference between GRBs located above and below the best fit  $E_{pi} - E_{iso}$  relation (see table 4).

## 6. Conclusions

We have studied the optical afterglows of 85 GRBs and have determined that the distribution of their optical brightness is mainly shaped by the intrinsic optical luminosity function. The extrinsic factors (redshift and visual extinction) seem to only behave as perturbations in this distribution. We also showed that optical selection effects act against the redshift measurement of faint GRBs in the rest frame, particularly for GRBs with  $L_R < 30.0 \log_{10}(erg.s^{-1}.Hz^{-1})$  and  $z < 1$ . These non optical detections prevent many GRBs from a redshift measurement. We also found a strong correlation between the location of the GRBs

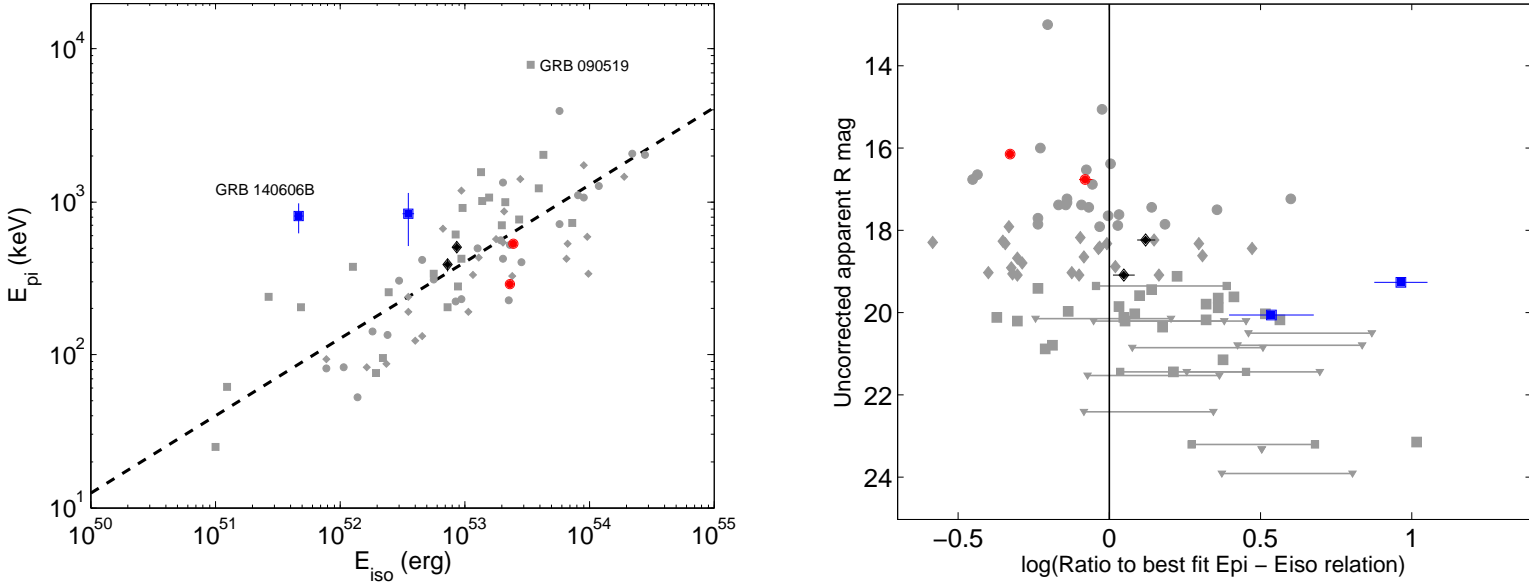


**Fig. 13.** Left panel : 6 Fermi GRBs from Singer et al. (2015) in the  $E_{\text{pi}} - E_{\text{iso}}$  plane. Right panel : The Fermi GRBs in the vertical distances/afterglow brightness plane. The colors and symbols show the class of the afterglow optical brightness (blue squares : faint afterglows, black diamonds : afterglow with intermediate brightness and red circles : bright afterglows).

**Table 4.** Result of the different statistical tests (Kolomogorov-Smirnov, bootstrap) when the 6 Fermi GRBs are taken into account in the analysis. The probabilities indicated correspond to the p-values, i.e, the probability of observing a test statistic as extreme as, or more extreme than, the observed value under the null hypothesis

Tested parameter	KS test (p-value)	Bootstrap test (p-value)
$\Delta Rmag_{\text{above/below}}^{\text{above}}$	$5.70 \times 10^{-6}$	$< 10^{-5}$
$\Delta dist_{\text{bright/faint}}^{\text{bright}}$	$1.73 \times 10^{-3}$	0.0021

with respect to the  $E_{\text{pi}} - E_{\text{iso}}$  relation and their afterglow optical brightnesses. This optical bias acts jointly with selection effects in the hard X-ray range against the detection of GRBs located well above the best fit  $E_{\text{pi}} - E_{\text{iso}}$  relation. Thus we conclude that the need to measure the redshift to obtain GRB rest-frame properties introduces significant biases in the observed distribution of GRBs in the  $E_{\text{pi}} - E_{\text{iso}}$  plane.

The complete understanding of the distribution of GRBs in the  $E_{\text{pi}} - E_{\text{iso}}$  plane and the connection with their afterglow emission will require detailed simulations of the GRB afterglow physics, of their luminosity function and their redshift distribution. The first point will be discussed in a future paper with the aim of providing clues about the connection between the prompt and afterglow physics of GRBs.

**Acknowledgements.** We gratefully acknowledge financial support from the OCEVU LabEx, France. We are also grateful to Yves Zolnierowski for insightful discussion.

## References

- Ackermann, M., Ajello, M., Asano, K., et al. 2013, *ApJ*, 763, 71
- Akitaya, H., Moritani, Y., Ui, T., Kanda, Y., & Yoshida, M. 2014, *GRB Coordinates Network*, 16163, 1
- Amati, L., Frontera, F., Tavani, M., et al. 2002, *A&A*, 390, 81
- Amati, L. & Valle, M. D. 2013, *International Journal of Modern Physics D*, 22, 30028
- Andreev, M., Sergeev, A., Parakhin, N., et al. 2009a, *GRB Coordinates Network*, 10273, 1
- Andreev, M., Sergeev, A., & Pozanenko, A. 2009b, *GRB Coordinates Network*, 10207, 1
- Anumapa, G. C., Gurugubelli, U. K., & Sahu, D. K. 2009, *GRB Coordinates Network*, 9576, 1
- Atteia, J.-L. 2003, *A&A*, 407, L1
- Band, D., Matteson, J., Ford, L., et al. 1993, *ApJ*, 413, 281
- Band, D. L. & Preece, R. D. 2005, *ApJ*, 627, 319
- Berger, E., Fox, D. B., Cucchiara, A., & Cenko, S. B. 2008, *GRB Coordinates Network*, 8335, 1
- Berger, E., Kulkarni, S. R., Bloom, J. S., et al. 2002, *ApJ*, 581, 981
- Berger, E. & Rauch, M. 2008, *GRB Coordinates Network*, 8542, 1

**Table 5.** Parameters of 71 GRBs with a redshift that make our sample. (1) GRB name, (2) redshift, (3) rest frame peak energy of the gamma-ray spectral energy distribution, (4) isotropic gamma-ray energy, (5)  $R_{mag}$  is the apparent R magnitude 2 hours after the burst not corrected from the galactic and host extinctions. (6)  $L_R^{rest}$  is the optical luminosity density taken 2 hours in the rest frame, (7) galactic extinction from Schlegel et al. (1998), (8) host extinction (\* indicates that the host extinction is estimated from the  $NH_{X,i}$  measurement), (9) vertical distance to the best fit  $E_{pi} - E_{iso}$  relation (dist; 0 if the GRB is below the best fit  $E_{pi} - E_{iso}$  relation and dist; 0 if it is above).

GRB	z	$E_{pi}$ (keV)	$E_{iso}$ ( $10^{52} erg$ )	$R_{mag}$ ( $t_{obs}=2h$ )	$\log_{10}(L_R^{rest})$ (erg/s/Hz)	$A_V^{Gal}$ (mag)	$A_V^{Host}$ (mag)	dist	Rf. z	Rf. $R_{mag}$
(1)	(2)	(3)	(4)	(5)	(6)	(7)	(8)	(9)	(10)	(11)
990123	1.60	2030.0 <sup>+161.0</sup> <sub>-161.0</sub>	278.0 <sup>+31.5</sup> <sub>-31.5</sub>	17.90	31.03	0.05	~ 0 <sup>a)</sup>	-0.029	A.	(1)
990510	1.619	423.0 <sup>+42.0</sup> <sub>-42.0</sub>	20.6 <sup>+2.9</sup> <sub>-2.9</sub>	17.40	31.58	0.66	0.22 <sup>a)</sup>	-0.1401	B.	(2)
990712	0.434	93.0 <sup>+15.0</sup> <sub>-15.0</sub>	0.78 <sup>+0.15</sup> <sub>-0.15</sub>	18.64	29.78	0.11	0.15 <sup>b)</sup>	-0.0810	C.	(3)
020124	3.198	339.6 <sup>+44.0</sup> <sub>-44.0</sub>	99.8 <sup>+21.0</sup> <sub>-21.0</sub>	18.29	31.29	0.16	0.28 <sup>a)</sup>	-0.5810	D.	(4) (5)
020813	1.25	592.9 <sup>+60.2</sup> <sub>-60.2</sub>	95.9 <sup>+3.6</sup> <sub>-3.6</sub>	17.91	30.99	0.36	0.12 <sup>a)</sup>	-0.3302	E.	(6) (7) (8) (9) (10) (11) (12) (13) (14)
021004	2.33	310.5 <sup>+84.0</sup> <sub>-84.0</sub>	5.68 <sup>+1.26</sup> <sub>-1.26</sub>	16.40	32.01	0.20	0.26 <sup>a)</sup>	0.0078	F.	(15) (16) (17) (18) (19)
021211	1.01	94.8 <sup>+6.8</sup> <sub>-6.8</sub>	2.23 <sup>+0.23</sup> <sub>-0.23</sub>	20.19	29.81	0.09	~ 0 <sup>a)</sup>	-0.3027	G.	(20) (21) (22) (23) (24) (25)
030328	1.52	327.3 <sup>+22.6</sup> <sub>-22.6</sub>	24.0 <sup>+0.73</sup> <sub>-0.73</sub>	18.79	30.66	0.15	~ 0 <sup>a)</sup>	-0.2849	H.	(26) (27) (28) (29) (30) (31)
030329	0.168	82.2 <sup>+1.5</sup> <sub>-1.5</sub>	1.07 <sup>+0.02</sup> <sub>-0.02</sub>	13.02	31.29	0.08	0.54 <sup>a)</sup>	-0.2038	I.	(32) (33)
040924	0.859	75.9 <sup>+2.5</sup> <sub>-2.5</sub>	1.96 <sup>+0.14</sup> <sub>-0.14</sub>	20.12	29.78	0.19	0.16 <sup>a)</sup>	-0.3710	J.	(34) (35) (36)
041006	0.716	82.2 <sup>+3.1</sup> <sub>-3.1</sub>	1.66 <sup>+0.05</sup> <sub>-0.05</sub>	18.68	30.35	0.71	0.11 <sup>a)</sup>	-0.3000	K.	(37) (38) (39)
050416A	0.6535	24.8 <sup>+3.8</sup> <sub>-4.5</sub>	0.10 <sup>+0.01</sup> <sub>-0.01</sub>	20.87	29.22	0.10	0.19 <sup>a)</sup>	-0.2087	L.	(40)
050525A	0.606	135.1 <sup>+2.7</sup> <sub>-2.7</sub>	2.41 <sup>+0.04</sup> <sub>-0.04</sub>	17.40	30.60	0.32	0.26 <sup>c)</sup>	-0.1656	M.	(41) (42) (43) (44) (45) (46) (47) (48) (49) (50) (51)
050820A	2.612	1326.7 <sup>+343.4</sup> <sub>-224.1</sub>	20.3 <sup>+1.43</sup> <sub>-1.43</sub>	17.51	31.61	0.15	0.065 <sup>d)</sup>	0.3595	N.	(52) (53)
050922C	2.198	417.5 <sup>+162.8</sup> <sub>-85.7</sub>	4.56 <sup>+0.15</sup> <sub>-0.15</sub>	17.87	31.36	0.34	0.07 <sup>e)</sup>	0.1844	O.	(54)
060115	3.53	280.9 <sup>+86.1</sup> <sub>-27.2</sub>	8.87 <sup>+0.78</sup> <sub>-0.78</sub>	19.97	30.88	0.44	~ 0 <sup>*</sup>	-0.1333	P.	(55) (56) (57)
060908	1.1884	425.3 <sup>+264.1</sup> <sub>-130.3</sub>	9.48 <sup>+0.38</sup> <sub>-0.38</sub>	19.85	30.08	0.12	0.09 <sup>a)</sup>	0.0324	Q.	(58)
061007	1.261	1065.4 <sup>+81.4</sup> <sub>-81.4</sub>	91.41 <sup>+1.16</sup> <sub>-1.16</sub>	17.44	31.21	0.07	0.66 <sup>f)</sup>	-0.0652	R.	(59)
061121	1.314	1402.3 <sup>+208.3</sup> <sub>-166.6</sub>	28.21 <sup>+0.41</sup> <sub>-0.41</sub>	18.63	30.72	0.15	0.28 <sup>a)</sup>	0.3116	S.	(60) (61) (62) (63) (64) (65) (66)
070612A	0.617	305.6 <sup>+95.4</sup> <sub>-73.4</sub>	3.0 <sup>+0.17</sup> <sub>-0.17</sub>	17.45	30.67	0.17	0.46 <sup>*</sup>	0.1409 <sup>*</sup>	T.	(67) (68) (69) (70) (71)
071010B	0.947	87.6 <sup>+1.4</sup> <sub>-1.4</sub>	2.35 <sup>+0.05</sup> <sub>-0.05</sub>	18.28	—	0.03	0.18 <sup>*</sup>	-0.3488	U.	(72) (73) (74) (75) (76)
071020	2.145	1014.3 <sup>+252.0</sup> <sub>-167.0</sub>	14.06 <sup>+0.61</sup> <sub>-0.61</sub>	19.81	30.61	0.21	0.28 <sup>a)</sup>	-0.3235	V.	(77) (78) (79) (80) (81)
080319B	0.937	1261.0 <sup>+27.1</sup> <sub>-27.1</sub>	120.36 <sup>+1.49</sup> <sub>-1.49</sub>	16.89	31.03	0.04	0.07 <sup>a)</sup>	-0.0523	W.	(82) (83)
080411	1.03	525.8 <sup>+71.2</sup> <sub>-54.8</sub>	23.24 <sup>+0.09</sup> <sub>-0.09</sub>	16.54	31.36	0.11	0.28 <sup>*</sup>	-0.0720	X.	(84) (85)
080413A	2.433	432.6 <sup>+449.7</sup> <sub>-144.2</sub>	12.97 <sup>+0.37</sup> <sub>-0.37</sub>	18.43	31.19	0.51	~ 0 <sup>d)</sup>	-0.0290	Y.	(86) (87) (88) (89) (90)
080413B	1.10	140.7 <sup>+27.3</sup> <sub>-16.8</sub>	1.85 <sup>+0.06</sup> <sub>-0.06</sub>	17.39	31.00	0.12	~ 0 <sup>a)</sup>	-0.0906	Z.	(91) (92)
080605	1.64	768.2 <sup>+198.0</sup> <sub>-198.0</sub>	27.60 <sup>+0.41</sup> <sub>-0.41</sub>	20.20	30.40	0.44	0.47 <sup>g)</sup>	0.0551	AA.	(93) (94) (95) (96) (97) (98) (99)
080721	2.591	1747.0 <sup>+241.3</sup> <sub>-742.5</sub>	91.00 <sup>+7.58</sup> <sub>-7.58</sub>	18.24	31.34	0.34	0.35 <sup>d)</sup>	0.1506	AB.	(100) (101) (102)
080804	2.2045	697.2 <sup>+78.4</sup> <sub>-78.4</sub>	19.80 <sup>+1.01</sup> <sub>-1.01</sub>	20.03	30.43	0.05	0.06 <sup>g)</sup>	0.0857	AC.	(103) (104) (105)
080810	3.355	3957.3 <sup>+801.7</sup> <sub>-801.7</sub>	58.58 <sup>+2.55</sup> <sub>-2.55</sub>	17.25	31.79	0.09	0.16 <sup>d)</sup>	0.6021	AD.	(106) (107) (108)
081007	0.5295	61.2 <sup>+15.3</sup> <sub>-15.3</sub>	0.12 <sup>+0.01</sup> <sub>-0.01</sub>	19.45	29.56	0.05	~ 0 <sup>a)</sup>	0.1403	AE.	(109)
081008	1.9685	493.3 <sup>+107.7</sup> <sub>-107.7</sub>	12.70 <sup>+0.59</sup> <sub>-0.59</sub>	17.62	31.59	0.31	0.46 <sup>a)</sup>	0.0326	AF.	(110) (111) (112) (113)
081121	2.512	564.6 <sup>+58.1</sup> <sub>-58.1</sub>	19.57 <sup>+1.43</sup> <sub>-1.43</sub>	17.65	31.52	0.17	0.13 <sup>*</sup>	-0.0034	AG.	(114) (115) (116)
081222	2.77	538.1 <sup>+36.1</sup> <sub>-36.1</sub>	20.28 <sup>+0.42</sup> <sub>-0.42</sub>	18.45	31.21	0.07	~ 0 <sup>a)</sup>	-0.321	AH.	(117) (118) (119) (120) (121) (122)
090102	1.543	1073.8 <sup>+45.9</sup> <sub>-45.9</sub>	15.96 <sup>+0.70</sup> <sub>-0.70</sub>	20.17	30.22	0.15	0.45 <sup>a)</sup>	0.3204	AI.	(123)
090418A	1.608	1567.4 <sup>+1444.8</sup> <sub>-560.7</sub>	13.75 <sup>+0.60</sup> <sub>-0.60</sub>	20.03	30.54	0.15	0.67 <sup>*</sup>	0.5174	AJ.	(124) (125) (126) (127) (128)
090423	8.26	613.9 <sup>+154.8</sup> <sub>-154.8</sub>	8.51 <sup>+0.58</sup> <sub>-0.58</sub>	21.45 <sup>*</sup>	—	0.10	~ 0 <sup>a)</sup>	0.2153	AK.	(129) (130) (131) (132) (133)
090424	0.544	237.1 <sup>+5.9</sup> <sub>-5.9</sub>	3.54 <sup>+0.35</sup> <sub>-0.35</sub>	18.33	30.15	0.08	0.50 <sup>d)</sup>	-0.0055	AL.	(134) (135) (136) (137) (138) (139) (140) (141) (142) (143) (144)
090516A	4.11	725.9 <sup>+135.2</sup> <sub>-135.2</sub>	73.95 <sup>+4.93</sup> <sub>-4.93</sub>	20.88 <sup>*</sup>	—	0.17	0.84 <sup>*</sup>	-0.1854	AM.	(145) (146) (147) (148) (149) (150)
090519	3.85	7848.2 <sup>+4282.6</sup> <sub>-4282.6</sub>	34.30 <sup>+2.86</sup> <sub>-2.86</sub>	23.14	29.77	0.13	0.01 <sup>g)</sup>	1.0167	AN.	(151) (152) (153) (154) (155) (156)
090618	0.54	226.2 <sup>+5.6</sup> <sub>-5.6</sub>	22.95 <sup>+0.22</sup> <sub>-0.22</sub>	16.65	30.83	0.28	0.25 <sup>a)</sup>	-0.4356	AO.	(157) (158) (159) (160) (161) (162) (163) (164) (165) (166) (167) (168) (169) (170)
090812	2.452	2022.9 <sup>+838.8</sup> <sub>-524.7</sub>	43.26 <sup>+1.49</sup> <sub>-1.49</sub>	21.15	30.18	0.08	0.41 <sup>g)</sup>	0.3771	AP.	(171) (172) (173) (174)
091020	1.71	661.9 <sup>+99.5</sup> <sub>-99.5</sub>	6.81 <sup>+0.18</sup> <sub>-0.18</sub>	18.31	31.01	0.06	0.36 <sup>*</sup>	0.2969	AQ.	(175) (176) (177) (178) (179) (180) (181)

Table 5. continued

GRB	z	$E_{pi}$ (keV)	$E_{iso}$ ( $10^{52} \text{ erg}$ )	$R_{mag}$ ( $t_{obs}=2\text{h}$ )	$\log_{10}(L_R^{rest})$ ( $\text{erg/s/Hz}$ )	$A_V^{Gal}$ (mag)	$A_V^{Host}$ (mag)	dist	Ref. z	Ref. $R_{mag}$
(1)	(2)	(3)	(4)	(5)	(6)	(7)	(8)	(9)	(10)	(11)
091029	2.752	$229.7^{+33.8}_{-94.5}$	$9.46^{+0.39}_{-0.39}$	17.85	31.44	0.06	$\sim 0^g$	-0.2348	AR.	(182) (183) (184) (185)
091127	0.49	$52.9^{+2.3}_{-2.3}$	$1.39^{+0.03}_{-0.05}$	16.77	30.60	0.13	0.11 <sup>a)</sup>	-0.4520	AS.	(186) (187) (188) (189) (190)
091208B	1.063	$255.4^{+41.4}_{-40.0}$	$2.50^{+0.15}_{-0.15}$	19.59	30.24	0.18	0.40 <sup>a)</sup>	0.1029	AT.	(191) (192) (193) (194) (195) (196)
100728B	2.106	$341.2^{+68.5}_{-68.5}$	$5.66^{+0.33}_{-0.33}$	20.11	30.53	0.22	0.35*	0.0495	AU.	(197) (198) (199) (200) (201)
100814A	1.44	$330.9^{+25.5}_{-25.5}$	$11.65^{+0.26}_{-0.26}$	19.02	30.59	0.07	0.11*	-0.1220	AV.	(202) (203) (204)
110205A	2.22	$714.8^{+238.3}_{-238.3}$	$57.82^{+3.78}_{-3.78}$	17.33	31.49	0.05	0.20 <sup>a)</sup>	-0.1382	AW.	(205) (206) (207) (208) (209)
110213A	1.46	$223.9^{+76.3}_{-64.0}$	$8.57^{+0.58}_{-0.58}$	16.02	32.14	1.06	0.07*	-0.2244	AX.	(210)
110422A	1.77	$421.0^{+13.9}_{-13.9}$	$66.04^{+1.61}_{-1.61}$	19.04	30.89	0.09	0.65*	-0.3972	AY.	(211) (212) (213)
110503A	1.613	$572.3^{+52.3}_{-49.3}$	$17.84^{+0.71}_{-0.71}$	18.89	30.68	0.08	0.15*	0.0227	AZ.	(214) (215) (216) (217) (218)
110731A	2.83	$1223.0^{+73.4}_{-73.4}$	$39.84^{+0.66}_{-0.66}$	20.36	30.72	0.57	0.24 <sup>a)</sup>	0.1766	BA.	(219) (220) (221) (222)
120326A	1.798	$122.9^{+10.8}_{-10.8}$	$4.08^{+0.47}_{-0.47}$	18.91	30.90	0.17	0.23*	-0.3222	BB.	(223) (224) (225) (226) (227)
120811C	2.671	$204.0^{+19.6}_{-19.6}$	$7.42^{+0.74}_{-0.74}$	19.42	30.94	0.11	0.53*	-0.2331	BC.	(228) (229) (230) (231) (232)
120907A	0.97	$241.2^{+67.3}_{-67.3}$	$0.27^{+0.04}_{-0.04}$	20.17	29.88	0.31	0.13*	0.5665	BD.	(233) (234) (235) (236) (237)
121211A	1.023	$202.8^{+32.0}_{-32.0}$	$0.49^{+0.10}_{-0.10}$	19.65	30.09	0.03	0.37*	0.3606	BE.	(238) (239) (240) (241)
130408A	3.758	$1003.9^{+138.0}_{-138.0}$	$21.39^{+3.72}_{-3.72}$	19.13	31.30	0.84	0.06*	0.2271	BF.	(242) (243) (244) (245)
130420A	1.297	$131.6^{+7.2}_{-7.2}$	$4.61^{+0.19}_{-0.19}$	19.06	30.51	0.04	0.21*	-0.3196	BG.	(246) (247)
130427A	0.3399	$1112.1^{+6.7}_{-6.7}$	$81.93^{+0.79}_{-0.79}$	15.08	30.96	0.07	0.11*	-0.0226	BH.	(248) (249) (250) (251) (252)
130505A	2.27	$2063.4^{+101.4}_{-101.4}$	$220.26^{+10.49}_{-10.49}$	17.89	31.42	0.13	0.35*	0.0293	BI.	(253) (254) (255) (256) (257)
130610A	2.092	$911.8^{+132.7}_{-132.7}$	$9.59^{+0.38}_{-0.38}$	19.88	30.53	0.07	0.23*	0.3609	BJ.	(258) (259) (260) (261)
130701A	1.155	$191.8^{+8.6}_{-8.6}$	$3.52^{+0.08}_{-0.08}$	19.08	30.43	0.28	0.09*	-0.0967	BK.	(262)
130831A	0.4791	$81.4^{+5.9}_{-5.9}$	$0.775^{+0.002}_{-0.002}$	17.23	30.39	0.15	0.07*	-0.1376	BL.	(263) (264) (265) (266)
131030A	1.293	$405.9^{+22.9}_{-22.9}$	$28.91^{+2.89}_{-2.89}$	17.70	31.04	0.19	0.21*	-0.2323	BM.	(267) (268) (269) (270)
140213A	1.2076	$191.2^{+7.8}_{-7.8}$	$10.75^{+1.07}_{-1.07}$	18.32	30.83	0.49	0.06*	-0.3423	BN.	(271) (272) (273) (274) (275)
140419A	3.956	$1452.1^{+416.3}_{-416.3}$	$191.66^{+19.17}_{-19.17}$	18.17	31.67	0.10	0.47*	-0.0928	BO.	(276) (277) (278) (279)
140423A	3.26	$532.5^{+38.3}_{-38.3}$	$67.97^{+2.17}_{-2.17}$	19.08	31.12	0.04	0.32*	-0.3015	BP.	(280) (281)
140506A	0.889	$373.2^{+61.5}_{-61.5}$	$1.28^{+0.14}_{-0.14}$	19.60	30.11	0.31	0.32*	0.4140	BQ.	(282) (283) (284) (285)
140512A	0.725	$1177.8^{+121.3}_{-121.3}$	$9.44^{+0.20}_{-0.20}$	18.44	30.41	0.53	0.10*	0.4755	BR.	(286) (287)
140703A	3.14	$861.3^{+148.3}_{-148.3}$	$20.96^{+1.61}_{-1.61}$	19.10	31.28	0.34	0.27*	0.1650	BS.	(288) (289) (290) (291) (292)
										(293) (294) (295)
										(296) (297) (298)
										(299) (300) (301) (302) (303)
										(304) (305) (306) (307) (308)
										(309) (310) (311) (312) (313)
										(314) (315)
										(316) (317) (318) (319) (320)
										(321) (322) (323) (324) (325)
										(326) (327) (328) (329) (330)
										(331)
										(332) (333)
										(334) (335) (336) (337) (338)
										(339) (340) (341) (342) (343)
										(344) (345) (346)
										(347) (348) (349) (350) (351)
										(352) (353) (354) (355) (356)
										(356) (357) (358) (359) (360)
										(361) (362)
										(363)
										(364) (365) (366) (367)
										(368)

Bersier, D. 2011, GRB Coordinates Network, 12216, 1

Bersier, D., Stanek, K. Z., Winn, J. N., et al. 2003, ApJ, 584, L43

Beskin, G., Birjukov, A., Koposov, S., Spiridonova, O., &amp; Pozanenko, A. 2002, GRB Coordinates Network, 1528, 1

Bikmaev, I., Khamitov, I., Melnikov, S., et al. 2014, GRB Coordinates Network, 16185, 1

Bikmaev, I., Zhuchkov, R., Sakhibullin, N., et al. 2009, GRB Coordinates Network, 9190, 1

Bloom, J. S., Perley, D. A., &amp; Chen, H. W. 2006, GRB Coordinates Network, 5826, 1

Bloom, J. S., Perley, D. A., Li, W., et al. 2009, ApJ, 691, 723

Brennan, T., Reichart, D., Nysewander, M., et al. 2008, GRB Coordinates Network, 7629, 1

Broens, E. &amp; Boyd, D. 2011, GRB Coordinates Network, 12009, 1

Burenin, R., Denissenko, D., Pavlinsky, M., et al. 2003, GRB Coordinates Network, 1990, 1

Butler, N., Watson, A. M., Kuttyrev, A., et al. 2012a, GRB Coordinates Network, 14077, 1

Butler, N., Watson, A. M., Kuttyrev, A., et al. 2012b, GRB Coordinates Network, 14080, 1



**Table 6.** The sample parameters of GRBs without a redshift. (1) GRB name, (2) and (3) minimum and maximum vertical distance to the best fit  $E_{\text{pi}} - E_{\text{iso}}$  plane respectively. (4) and (5) redshift at the minimum and maximum distance to the best fit  $E_{\text{pi}} - E_{\text{iso}}$  relation. For GRB 051008 we used the strong constraint on redshift determined by Volnova et al. (2014i). (6) and (7) rest frame peak energy of the gamma-ray spectral energy distribution at the minimum and maximum distance to the best fit  $E_{\text{pi}} - E_{\text{iso}}$  relation, respectively. (8) and (9) isotropic gamma-ray energy at the minimum and maximum distance to the best fit  $E_{\text{pi}} - E_{\text{iso}}$  relation, respectively. (10)  $R_{\text{mag}}$  is the apparent R magnitude 2 hours after the burst not corrected from the galactic and host extinctions ( $\dagger$ : calibrated with the V-band magnitude).

GRB	dmin	dmax	$z_{\text{dmin}}$	$z_{\text{dmax}}$	$E_{\text{pi}}^{\text{dmin}}$ (keV)	$E_{\text{pi}}^{\text{dmax}}$ (keV)	$E_{\text{iso}}^{\text{dmin}}$ ( $10^{52}$ erg)	$E_{\text{iso}}^{\text{dmax}}$ ( $10^{52}$ erg)	$R_{\text{mag}}$ ( $t_{\text{obs}}=2\text{h}$ )	Ref. $R_{\text{mag}}$
(1)	(2)	(3)	(4)	(5)	(6)	(7)	(8)	(9)	(10)	(11)
051008	0.5051	0.5056	2.84	2.62	3317.8	3131.3	64.33	0.95	23.30*	(372) (373) (374)
060105	-0.0496	0.3812	3.40	0.3399	1437.3	438.1	154.15	57.09	20.20*	(375) (376) (377)
060117	-0.2439	0.2050	3.72	0.3399	867.9	246.5	137.66	2.04	20.15*	(378)
060904	-0.0707	0.3652	3.56	0.3399	742.6	218.4	45.81	1.46	21.51*	(379) (380) (381)
090813	0.0458	0.4526	3.15	0.3399	394.3	127.3	7.68	0.55	20.21*	(382) (383)
091221	0.0378	0.4557	3.24	0.3399	878.6	277.4	38.96	0.13	21.44	(384) (385) (386)
100413A	0.4256	0.8369	3.15	0.3399	1232.1	397.4	12.97	0.59	23.20	(387) (388) (389) (390)
101011A	0.2738	0.6830	3.07	0.3399	1816.9	597.6	56.02	0.21	20.80 $\dagger$	(391) (392) (393) (394)
140102A	-0.0407	0.3890	3.40	0.3399	817.5	249.2	48.35	0.64	19.34	(395) (396) (397) (398) (399)
										(400) (401) (402) (403)
140626A	0.0796	0.5119	3.47	0.3399	200.0	59.9	1.71	0.02	20.84*	(404) (405)
140709B	0.4601	0.8719	3.15	0.3399	2201.7	710.1	35.02	0.57	20.50*	(406) (407) (408)
140713A	0.3737	0.8044	3.48	0.3399	429.7	128.6	2.03	0.03	23.90*	(409) (410)
141005A	0.2597	0.6998	3.64	0.3399	551.7	159.4	5.62	0.06	21.44*	(411) (412)
141017A	-0.0806	0.3469	3.39	0.3399	426.3	130.0	15.95	0.22	22.40*	(413) (414)

- Butler, N., Watson, A. M., Kutyrev, A., et al. 2013a, GRB Coordinates Network, 14431, 1
- Butler, N., Watson, A. M., Kutyrev, A., et al. 2013b, GRB Coordinates Network, 14441, 1
- Butler, N., Watson, A. M., Kutyrev, A., et al. 2013c, GRB Coordinates Network, 15165, 1
- Butler, N., Watson, A. M., Kutyrev, A., et al. 2014a, GRB Coordinates Network, 16121, 1
- Butler, N., Watson, A. M., Kutyrev, A., et al. 2014b, GRB Coordinates Network, 16174, 1
- Butler, N., Watson, A. M., Kutyrev, A., et al. 2014c, GRB Coordinates Network, 16513, 1
- Butler, N. R., Bloom, J. S., & Poznanski, D. 2010, ApJ, 711, 495
- Butler, N. R., Kocevski, D., & Bloom. 2009, ApJ, 694, 76
- Butler, N. R., Kocevski, D., Bloom, J. S., & Curtis, J. L. 2007, ApJ, 671, 656
- Cabrera, J. I., Firmani, C., Avila-Reese, V., et al. 2007, MNRAS, 382, 342
- Cano, Z., de Ugarte Postigo, A., Pozanenko, A., et al. 2014a, A&A, 568, A19
- Cano, Z., Guidorzi, C., Bersier, D., et al. 2009a, GRB Coordinates Network, 9531, 1
- Cano, Z., Malesani, D., Geier, S., et al. 2014b, GRB Coordinates Network, 16169, 1
- Cano, Z., Melandri, A., Mundell, C. G., et al. 2009b, GRB Coordinates Network, 10262, 1
- Castro-Tirado, A. J., Cunniffe, R., Sanchez-Ramirez, R., et al. 2014, GRB Coordinates Network, 16505, 1
- Castro-Tirado, A. J., Möller, P., García-Segura, G., et al. 2010, A&A, 517, A61
- Cenko, S. B. 2009a, GRB Coordinates Network, 9201, 1
- Cenko, S. B. 2009b, GRB Coordinates Network, 9513, 1
- Cenko, S. B., Cucchiara, A., Fox, D. B., Berger, E., & Price, P. A. 2007a, GRB Coordinates Network, 6888, 1
- Cenko, S. B., Fox, D. B., Cucchiara, A., et al. 2007b, GRB Coordinates Network, 6556, 1
- Cenko, S. B., Hora, J. L., & Bloom, J. S. 2011, GRB Coordinates Network, 11638, 1
- Cenko, S. B., Kasliwal, M., Harrison, F. A., et al. 2006, ApJ, 652, 490
- Cenko, S. B., Kulkarni, S. R., Gal-Yam, A., & Berger, E. 2005, GRB Coordinates Network, 3542, 1
- Cenko, S. B. & Perley, D. A. 2013a, GRB Coordinates Network, 14846, 1
- Cenko, S. B. & Perley, D. A. 2013b, GRB Coordinates Network, 14960, 1
- Cenko, S. B. & Perley, D. A. 2014a, GRB Coordinates Network, 16129, 1
- Cenko, S. B. & Perley, D. A. 2014b, GRB Coordinates Network, 16153, 1
- Cenko, S. B., Perley, D. A., Jankkarinen, V., et al. 2009, GRB Coordinates Network, 9518, 1
- Cenko, S. B. & Rau, A. 2006, GRB Coordinates Network, 5512, 1
- Chen, T.-W., Huang, L.-C., Chen, Y.-T., et al. 2008, GRB Coordinates Network, 7990, 1
- Chen, Y. T., King, S. K., Wen, C. Y., et al. 2014, GRB Coordinates Network, 15877, 1
- Choi, C., Im, M., Sung, H.-I., & Urata, Y. 2014a, GRB Coordinates Network, 16149, 1
- Choi, C., Im, M., Sung, H.-I., & Urata, Y. 2014b, GRB Coordinates Network, 15689, 1
- Chornock, R., Cenko, S. B., Griffith, C. V., et al. 2009a, GRB Coordinates Network, 9151, 1
- Chornock, R., Cenko, S. B., Li, W., & Filippenko, A. V. 2009b, GRB Coordinates Network, 9148, 1
- Chornock, R., Perley, D. A., Cenko, S. B., & Bloom, J. S. 2009c, GRB Coordinates Network, 9243, 1
- Chornock, R., Perley, D. A., & Cobb, B. E. 2009d, GRB Coordinates Network, 10100, 1
- Christensen, L., Hjorth, J., Gorosabel, J., et al. 2004, A&A, 413, 121
- Christie, G. W., de Ugarte Postigo, A., & Natusch, T. 2009a, GRB Coordinates Network, 9396, 1
- Christie, G. W., Dong, S., de Ugarte Postigo, A., & Natusch, T. 2009b, GRB Coordinates Network, 10137, 1
- Ciabattari, F., Donati, S., Mazzoni, E., Petroni, G., & Rossi, M. 2014, GRB Coordinates Network, 16511, 1
- Cobb, B. E. 2008a, GRB Coordinates Network, 7609, 1
- Cobb, B. E. 2008b, GRB Coordinates Network, 8356, 1
- Cobb, B. E. 2008c, GRB Coordinates Network, 8547, 1
- Cobb, B. E. & Bailyn, C. D. 2005, GRB Coordinates Network, 3506, 1
- Cobb, B. E., Bloom, J. S., Perley, D. A., et al. 2010, ApJ, 718, L150
- Collazzi, A. C., Schaefer, B. E., Goldstein, A., & Preece, R. D. 2012, ApJ, 747, 39
- Covino, S., Campana, S., Conciatore, M. L., et al. 2010, A&A, 521, A53
- Covino, S., Melandri, A., Salvaterra, R., et al. 2013, MNRAS, 432, 1231
- Coward, D., Howell, E., Wan, L., & Macpherson, D. 2014, ArXiv e-prints
- Cucchiara, A., Cenko, S. B., Bloom, J. S., et al. 2011a, ApJ, 743, 154
- Cucchiara, A., Fox, D., Levan, A., & Tanvir, N. 2009, GRB Coordinates Network, 10202, 1
- Cucchiara, A. & Fox, D. B. 2009, GRB Coordinates Network, 8774, 1
- Cucchiara, A., Fox, D. B., Cenko, S. B., & Berger, E. 2008a, GRB Coordinates Network, 8372, 1
- Cucchiara, A., Fox, D. B., Cenko, S. B., & Berger, E. 2008b, GRB Coordinates

- Network, 8346, 1
- Cucchiara, A., Fox, D. B., Cenko, S. B., & Berger, E. 2008c, GRB Coordinates Network, 8713, 1
- Cucchiara, A., Fox, D. B., Cenko, S. B., & Berger, E. 2008d, GRB Coordinates Network, 8065, 1
- Cucchiara, A., Levan, A. J., Fox, D. B., et al. 2011b, *ApJ*, 736, 7
- Cucchiara, A. & Perley, D. 2013, GRB Coordinates Network, 15144, 1
- Cwiok, M., Dominik, W., Kaspruwicz, G., et al. 2008, GRB Coordinates Network, 8707, 1
- D'Avanzo, P., D'Elia, V., di Fabrizio, L., & Gurtu, A. 2011, GRB Coordinates Network, 11997, 1
- De Cia, A., Malesani, D., Vreeswijk, P. M., Schulze, S., & Jakobsson, P. 2010, GRB Coordinates Network, 11027, 1
- de Pasquale, M. & Cannizzo, J. 2010, GRB Coordinates Network, 11338, 1
- de Ugarte Postigo, A., Castro-Tirado, A. J., Gorosabel, J., et al. 2005, *A&A*, 443, 841
- de Ugarte Postigo, A., Castro-Tirado, A. J., Tello, J. C., Cabrera Lavers, A., & Reverte, D. 2011, GRB Coordinates Network, 11993, 1
- de Ugarte Postigo, A., Gorosabel, J., D'Avanzo, P., et al. 2009a, GRB Coordinates Network, 10104, 1
- de Ugarte Postigo, A., Gorosabel, J., Fynbo, J. P. U., Wiersema, K., & Tanvir, N. 2009b, GRB Coordinates Network, 9771, 1
- de Ugarte Postigo, A., Gorosabel, J., Malesani, D., Fynbo, J. P. U., & Levan, A. J. 2009c, GRB Coordinates Network, 9381, 1
- de Ugarte Postigo, A., Gorosabel, J., Malesani, D., Fynbo, J. P. U., & Levan, A. J. 2009d, GRB Coordinates Network, 9383, 1
- de Ugarte Postigo, A., Gorosabel, J., Xu, D., et al. 2014a, GRB Coordinates Network, 16253, 1
- de Ugarte Postigo, A., Gorosabel, J., Xu, D., et al. 2014b, GRB Coordinates Network, 16310, 1
- de Ugarte Postigo, A., Tanvir, N., Sanchez-Ramirez, R., et al. 2013, GRB Coordinates Network, 14437, 1
- Della Valle, M., Benetti, S., Malesani, D., et al. 2003, GRB Coordinates Network, 1809, 1
- Dereli, H., Klotz, A., Macpherson, D., et al. 2013, GRB Coordinates Network, 14372, 1
- Distefano, E., Covino, S., Molinari, E., et al. 2006, GRB Coordinates Network, 4526, 1
- Durig, D. T., Oksanen, A. C., Pullen, C., & Price, A. 2005, GRB Coordinates Network, 3478, 1
- Eichler, D. & Levinson, A. 2004, *ApJ*, 614, L13
- Elenin, L., Molotov, I., & Pozanenko, A. 2010, GRB Coordinates Network, 11012, 1
- Elenin, L., Savanevych, V., Bryukhovetskiy, A., Molotov, I., & Pozanenko, A. 2013a, GRB Coordinates Network, 14860, 1
- Elenin, L., Volnova, A., Molotov, I., & Pozanenko, A. 2012, GRB Coordinates Network, 13679, 1
- Elenin, L., Volnova, A., Molotov, I., & Pozanenko, A. 2014, GRB Coordinates Network, 16148, 1
- Elenin, L., Volnova, A., Savanevych, V., et al. 2013b, GRB Coordinates Network, 14428, 1
- Elliott, J., Varela, K., Kann, D. A., & Greiner, J. 2014, GRB Coordinates Network, 15829, 1
- Elunko, E. & Pozanenko, A. 2011, GRB Coordinates Network, 11958, 1
- Fatkullin, T., Moskvitin, A., Castro-Tirado, A. J., & de Ugarte Postigo, A. 2009, GRB Coordinates Network, 9542, 1
- Fernandez-Soto, A., Peris, V., & Alonso-Lorite, J. 2009, GRB Coordinates Network, 9536, 1
- Ferrante, F. V., Guver, T., Flewelling, H., Kehoe, R., & Dhungana, G. 2014, GRB Coordinates Network, 16145, 1
- Filgas, R., Afonso, P., Klose, S., & Greiner, J. 2009a, GRB Coordinates Network, 10286, 1
- Filgas, R., Greiner, J., Schady, P., et al. 2011, *A&A*, 535, A57
- Filgas, R., Kruehler, T., Greiner, J., & Yoldas, A. 2010, GRB Coordinates Network, 10592, 1
- Filgas, R., Updike, A., & Greiner, J. 2009b, GRB Coordinates Network, 10098, 1
- Fiore, F., Savaglio, S., Antonelli, L. A., et al. 2002, GRB Coordinates Network, 1524, 1
- Firmani, C., Cabrera, J. I., Avila-Reese, V., et al. 2009, *MNRAS*, 393, 1209
- Flores, H., Covino, S., Xu, D., et al. 2013, GRB Coordinates Network, 14491, 1
- Flores, H., Fynbo, J. P. U., de Ugarte Postigo, A., et al. 2010, GRB Coordinates Network, 11317, 1
- Foley, R. J., Chen, H.-W., Bloom, J., & Prochaska, J. X. 2005, GRB Coordinates Network, 3483, 1
- Fox, D. W., Price, P. A., Soderberg, A. M., et al. 2003, *ApJ*, 586, L5
- Fugazza, D., Antonelli, L. A., Fiore, F., et al. 2003, GRB Coordinates Network, 1982, 1
- Fujiwara, T., Yoshii, T., Saito, Y., et al. 2014, GRB Coordinates Network, 16173, 1
- Fynbo, J. P. U., Jakobsson, P., Prochaska, J. X., et al. 2009, *ApJS*, 185, 526
- Fynbo, J. P. U., Krühler, T., Leighly, K., et al. 2014, *A&A*, 572, A12
- Galama, T. J., Vreeswijk, P. M., Rol, E., et al. 1999, GRB Coordinates Network, 388, 1
- Galeev, A., Bikmaev, I., Sakhibullin, N., et al. 2009, GRB Coordinates Network, 9548, 1
- Galeev, A., Khamitov, I., Bikmaev, I., et al. 2012a, GRB Coordinates Network, 13626, 1
- Galeev, A., Khamitov, I., Bikmaev, I., et al. 2012b, GRB Coordinates Network, 13636, 1
- Garnavich, P. & Quinn, J. 2002, GRB Coordinates Network, 1661, 1
- Gendre, B., Atteia, J. L., Boër, M., et al. 2012, *ApJ*, 748, 59
- Gendre, B., Klotz, A., Palazzi, E., et al. 2010, *MNRAS*, 405, 2372
- Ghirlanda, G., Ghisellini, G., & Firmani, C. 2005, *MNRAS*, 361, L10
- Goldstein, A. 2012, in *Gamma-Ray Bursts 2012 Conference (GRB 2012)*
- Gomboc, A., Guidorzi, C., Melandri, A., et al. 2008a, GRB Coordinates Network, 7625, 1
- Gomboc, A., Guidorzi, C., Melandri, A., et al. 2008b, GRB Coordinates Network, 7626, 1
- Gomboc, A., Melandri, A., Smith, R. J., et al. 2008c, GRB Coordinates Network, 7831, 1
- Gorbovskey, E., Lipunov, V., Denisenko, D., et al. 2013, GRB Coordinates Network, 15405, 1
- Gorbovskey, E., Lipunov, V., Kornilov, V., et al. 2009, GRB Coordinates Network, 10231, 1
- Gorbovskey, E., Lipunov, V., Kornilov, V., et al. 2014, GRB Coordinates Network, 16250, 1
- Gorosabel, J., Castro-Tirado, A. J., Ramirez-Ruiz, E., et al. 2006, *ApJ*, 641, L13
- Gorosabel, J., de Ugarte Postigo, A., Montes, D., Kluttsch, A., & Castro-Tirado, A. J. 2009a, GRB Coordinates Network, 9379, 1
- Gorosabel, J., Fynbo, J. P. U., Hjorth, J., et al. 2002, GRB Coordinates Network, 1651, 1
- Gorosabel, J., Kubanek, P., Jelinek, M., de Ugarte Postigo, A., & Aceituno, J. 2009b, GRB Coordinates Network, 9236, 1
- Graham, J., Varela, K., Delvaux, C., & Greiner, J. 2014, GRB Coordinates Network, 16257, 1
- Granot, J. & Sari, R. 2002, *ApJ*, 568, 820
- Greiner, J., Krühler, T., Klose, S., et al. 2011, *A&A*, 526, A30
- Gruber, D., Goldstein, A., Weller von Ahlefeld, V., et al. 2014, *ApJS*, 211, 12
- Gruber et al. 2012, *ArXiv e-prints*, arXiv:1207.4620
- Guidorzi, C. & Melandri, A. 2013, GRB Coordinates Network, 15140, 1
- Guidorzi, C., Melandri, A., Kopac, D., & Gomboc, A. 2013, GRB Coordinates Network, 14405, 1
- Guidorzi, C., Smith, R. J., Tanvir, N., et al. 2010, GRB Coordinates Network, 10589, 1
- Guidorzi, C. & Steele, I. 2008, GRB Coordinates Network, 8064, 1
- Guidorzi, C., Steele, I. A., Melandri, A., et al. 2009, GRB Coordinates Network, 9375, 1
- Guver, T. 2013, GRB Coordinates Network, 14407, 1
- Guver, T., Ferrante, F. V., Flewelling, H., Kehoe, R., & Dhungana, G. 2014, GRB Coordinates Network, 16120, 1
- Guziy, S., Gorosabel, J., Castro-Tirado, A. J., et al. 2014, GRB Coordinates Network, 15685, 1
- Haislip, J., MacLeod, C., Nysewander, M., et al. 2005, GRB Coordinates Network, 3568, 1
- Haislip, J., Reichart, D., Ivarsen, K., et al. 2009a, GRB Coordinates Network, 9999, 1
- Haislip, J., Reichart, D., Ivarsen, K., et al. 2009b, GRB Coordinates Network, 10219, 1
- Haislip, J., Reichart, D., Ivarsen, K., et al. 2009c, GRB Coordinates Network, 10230, 1
- Haislip, J., Reichart, D., Ivarsen, K., et al. 2009d, GRB Coordinates Network, 10294, 1
- Halpern, J. & Armstrong, E. 2006a, GRB Coordinates Network, 5853, 1
- Halpern, J. & Armstrong, E. 2006b, GRB Coordinates Network, 5851, 1
- Halpern, J. P., Mirabal, N., & Armstrong, E. 2006, GRB Coordinates Network, 5847, 1
- Harbeck, D., Kaur, A., Delgado-Navarro, A., Orío, M., & Hartmann, D. H. 2014a, GRB Coordinates Network, 16165, 1
- Harbeck, D., Kaur, A., Delgado-Navarro, A., Orío, M., & Hartmann, D. H. 2014b, GRB Coordinates Network, 16175, 1
- Harrison, F. A., Bloom, J. S., Frail, D. A., et al. 1999, *ApJ*, 523, L121
- Henden, A., Gross, J., Denny, B., Terrell, D., & Cooney, W. 2009a, GRB Coordinates Network, 9220, 1
- Henden, A., Gross, J., Denny, B., Terrell, D., & Cooney, W. 2009b, GRB Coordinates Network, 9211, 1

- Hentunen, V.-P. 2007, GRB Coordinates Network, 6981, 1
- Hentunen, V.-P. & Nissinen, M. 2013, GRB Coordinates Network, 14891, 1
- Hentunen, V.-P., Nissinen, M., & Salmi, T. 2011a, GRB Coordinates Network, 11709, 1
- Hentunen, V.-P., Nissinen, M., & Salmi, T. 2011b, GRB Coordinates Network, 11966, 1
- Hentunen, V.-P., Nissinen, M., & Salmi, T. 2012, GRB Coordinates Network, 13119, 1
- Hentunen, V.-P., Nissinen, M., & Salmi, T. 2013a, GRB Coordinates Network, 14410, 1
- Hentunen, V.-P., Nissinen, M., & Salmi, T. 2013b, GRB Coordinates Network, 14572, 1
- Hentunen, V.-P., Nissinen, M., & Salmi, T. 2013c, GRB Coordinates Network, 15418, 1
- Hentunen, V.-P., Nissinen, M., & Salmi, T. 2014, GRB Coordinates Network, 16126, 1
- Hentunen, V.-P., Nissinen, M., Salmi, T., & Vilokki, H. 2011c, GRB Coordinates Network, 11717, 1
- Hentunen, V.-P., Nissinen, M., Vilokki, H., & Salmi, T. 2013d, GRB Coordinates Network, 15156, 1
- Heussaff, V., Atteia, J.-L., & Zolnierowski, Y. 2013, A&A, 557, A100
- Hjorth, J., Malesani, D., Jakobsson, P., et al. 2012, ApJ, 756, 187
- Hjorth, J., Melandri, A., Malesani, D., Kruehler, T., & Xu, D. 2013, GRB Coordinates Network, 14365, 1
- Hjorth, J., Möller, P., Gorosabel, J., et al. 2003, ApJ, 597, 699
- Holland, S. T., Bersier, D., Bloom, J. S., et al. 2004, AJ, 128, 1955
- Holland, S. T., Weidinger, M., Fynbo, J. P. U., et al. 2003, AJ, 125, 2291
- Huang, K. Y., Urata, Y., Filippenko, A. V., et al. 2005, ApJ, 628, L93
- Huang, L.-C., Chen, T.-W., Chen, Y.-T., Huang, K. Y., & Urata, Y. 2008, GRB Coordinates Network, 7999, 1
- Ibrahimov, M. A., Asfandiyarov, I. M., Kahharov, B. B., et al. 2003, GRB Coordinates Network, 2192, 1
- Im, M. & Choi, C. 2013, GRB Coordinates Network, 15432, 1
- Im, M., Lee, I., & Urata, Y. 2007, GRB Coordinates Network, 6970, 1
- Im, M., Park, W., Jeon, Y., et al. 2009a, GRB Coordinates Network, 9248, 1
- Im, M., Park, W. K., & Urata, Y. 2009b, GRB Coordinates Network, 9522, 1
- Im, M., Sung, H.-I., & Urata, Y. 2011, GRB Coordinates Network, 12004, 1
- Im, M., Sung, H.-I., & Urata, Y. 2013, GRB Coordinates Network, 14854, 1
- Ishimura, T., Yatsu, Y., Shimokawabe, T., Kawai, N., & Yoshida, M. 2007, GRB Coordinates Network, 7026, 1
- Ivanov, K., Yazev, S., Budnev, N. M., et al. 2014, GRB Coordinates Network, 16552, 1
- Ivanov, K., Yazev, S., Budnev, N. M., et al. 2010, GRB Coordinates Network, 10582, 1
- Izzo, L. & D'Avino, L. 2013, GRB Coordinates Network, 15153, 1
- Jakobsson, P., Fynbo, J. P. U., Paraficz, D., et al. 2005, GRB Coordinates Network, 4029, 1
- Jakobsson, P., Malesani, D., Vreeswijk, P. M., et al. 2008a, GRB Coordinates Network, 7998, 1
- Jakobsson, P., Vreeswijk, P. M., Hjorth, J., et al. 2007, GRB Coordinates Network, 6952, 1
- Jakobsson, P., Vreeswijk, P. M., Xu, D., & Thoene, C. C. 2008b, GRB Coordinates Network, 7832, 1
- Jang, M., Im, M., & Urata, Y. 2012, GRB Coordinates Network, 13139, 1
- Japelj, J., Kopac, D., Guidorzi, C., Mundell, C., & Virgili, F. 2012, GRB Coordinates Network, 14058, 1
- Japelj, J., Kopač, D., Kobayashi, S., et al. 2014, ApJ, 785, 84
- Jelinek, M. & Kubanek, P. 2009, GRB Coordinates Network, 9404, 1
- Jeon, Y., Im, M., Pak, S., & Jeong, H. 2011, GRB Coordinates Network, 11967, 1
- Jin, Z.-P., Covino, S., Della Valle, M., et al. 2013, ApJ, 774, 114
- Kaneko, Y., Ramirez-Ruiz, E., Granot, J., et al. 2007, ApJ, 654, 385
- Kann, D. A., Hoegner, C., & Filgas, R. 2007, GRB Coordinates Network, 6918, 1
- Kann, D. A., Klose, S., Zhang, B., et al. 2010, ApJ, 720, 1513
- Kann, D. A., Laux, U., & Ertel, S. 2008, GRB Coordinates Network, 7845, 1
- Kann, D. A., Laux, U., Roeder, M., & Meusinger, H. 2009a, GRB Coordinates Network, 10076, 1
- Kann, D. A., Laux, U., Roeder, M., & Meusinger, H. 2009b, GRB Coordinates Network, 10090, 1
- Kann, D. A. & Manohar, S. 2006, GRB Coordinates Network, 5278, 1
- Kann, D. A., Nicuesa Guelbenzu, A., & Greiner, J. 2014, GRB Coordinates Network, 16926, 1
- Kann, D. A., Schmidl, S., Hoegner, C., et al. 2011, GRB Coordinates Network, 11996, 1
- Kann, D. A., Stecklum, B., & Ludwig, F. 2013, GRB Coordinates Network, 14593, 1
- Khamitov, I., Parmaksizoglu, M., Ak, T., et al. 2009, GRB Coordinates Network, 9597, 1
- Khorunzhev, G., Burenin, R., Pavlinsky, M., et al. 2013, GRB Coordinates Network, 15244, 1
- Kinugasa, K., Honda, S., Hashimoto, O., Takahashi, H., & Taguchi, H. 2009a, GRB Coordinates Network, 10248, 1
- Kinugasa, K., Honda, S., Takahashi, H., Taguchi, H., & Hashimoto, O. 2009b, GRB Coordinates Network, 10275, 1
- Kiziloglu, U., Alpar, A., Baykal, A., et al. 2002, GRB Coordinates Network, 1488, 1
- Klotz, A., Boer, M., & Atteia, J. L. 2006, GRB Coordinates Network, 5506, 1
- Klotz, A., Boer, M., & Atteia, J. L. 2008, GRB Coordinates Network, 7595, 1
- Klotz, A., Boer, M., Atteia, J. L., et al. 2005, A&A, 439, L35
- Klotz, A., Gendre, B., Boer, M., & Atteia, J. L. 2009a, GRB Coordinates Network, 9401, 1
- Klotz, A., Gendre, B., Boer, M., & Atteia, J. L. 2009b, GRB Coordinates Network, 10200, 1
- Klotz, A., Gendre, B., Boer, M., & Atteia, J. L. 2011, GRB Coordinates Network, 12011, 1
- Klotz, A., Gendre, B., Boer, M., & Atteia, J. L. 2012, GRB Coordinates Network, 13108, 1
- Klotz, A., Gendre, B., Boer, M., et al. 2013, GRB Coordinates Network, 14908, 1
- Klotz, A. & Kugel, F. 2009, GRB Coordinates Network, 9402, 1
- Klotz, A., Turpin, D., Boer, M., et al. 2014a, GRB Coordinates Network, 16469, 1
- Klotz, A., Turpin, D., MacPherson, D., et al. 2014b, GRB Coordinates Network, 16920, 1
- Klunko, E., Volnova, A., Eselevich, M., Korobtsev, I., & Pozanenko, A. 2014, GRB Coordinates Network, 16251, 1
- Klunko, E., Volnova, A., & Pozanenko, A. 2009, GRB Coordinates Network, 9613, 1
- Kobayashi, S. 2000, ApJ, 545, 807
- Kocevski, D. 2012, ApJ, 747, 146
- Kocevski, D., Perley, D. A., Bloom, J. S., Modjaz, M., & Poznanski, D. 2007, GRB Coordinates Network, 6919, 1
- Krimm, H. A., Yamaoka, K., Sugita, S., et al. 2009, ApJ, 704, 1405
- Kruehler, T., Kupcu Yoldas, A., Greiner, J., et al. 2008a, GRB Coordinates Network, 7586, 1
- Kruehler, T., Schrey, F., Greiner, J., et al. 2008b, GRB Coordinates Network, 8075, 1
- Krugly, Y., Slyusarev, I., Molotov, I., & Pozanenko, A. 2013, GRB Coordinates Network, 14585, 1
- Kulkarni, S. R., Djorgovski, S. G., Odewahn, S. C., et al. 1999, Nature, 398, 389
- Kumar, P. & Zhang, B. 2014, ArXiv e-prints
- Kuroda, D., Hanayama, H., Miyaji, T., et al. 2011a, GRB Coordinates Network, 11972, 1
- Kuroda, D., Hanayama, H., Miyaji, T., et al. 2011b, GRB Coordinates Network, 12226, 1
- Kuroda, D., Hanayama, H., Miyaji, T., et al. 2014a, GRB Coordinates Network, 16132, 1
- Kuroda, D., Yanagisawa, K., Shimizu, H., et al. 2011c, GRB Coordinates Network, 11719, 1
- Kuroda, D., Yanagisawa, K., Shimizu, Y., et al. 2012, GRB Coordinates Network, 14062, 1
- Kuroda, D., Yanagisawa, K., Shimizu, Y., et al. 2013, GRB Coordinates Network, 14568, 1
- Kuroda, D., Yanagisawa, K., Shimizu, Y., et al. 2014b, GRB Coordinates Network, 16131, 1
- Kuroda, D., Yanagisawa, K., Shimizu, Y., et al. 2014c, GRB Coordinates Network, 16160, 1
- Kuroda, D., Yoshida, M., Yanagisawa, K., et al. 2008, GRB Coordinates Network, 8724, 1
- Kuvshinov, D., Lipunov, V., Kornilov, V., et al. 2008, GRB Coordinates Network, 7836, 1
- Laas-Bourez, M., Coward, D., Blair, D., et al. 2010, GRB Coordinates Network, 11336, 1
- Lamb, D. Q., Donaghy, T. Q., & Graziani, C. 2005, ApJ, 620, 355
- Laursen, L. T. & Stanek, K. Z. 2003, ApJ, 597, L107
- Lee, I., Im, M., & Urata, Y. 2010, Journal of Korean Astronomical Society, 43, 95
- Lee, W. H., Butler, N., Watson, A. M., et al. 2013, GRB Coordinates Network, 15321, 1
- Leloudas, G., Tanvir, N. R., Xu, D., et al. 2013, GRB Coordinates Network, 14954, 1
- Leloudas, G., Xu, D., de Ugarte Postigo, A., et al. 2011, GRB Coordinates Network, 11994, 1
- Leonini, S., Guerrini, G., Rosi, P., & Tinjaca Ramirez, L. M. 2013, GRB Coordinates Network, 15150, 1

- Li, W., Filippenko, A. V., Chornock, R., & Jha, S. 2003, *ApJ*, 586, L9
- Li, W., Perley, D. A., & Filippenko, A. V. 2009, GRB Coordinates Network, 9517, 1
- Li, W. D., Filippenko, A. V., & Chornock, R. 2002a, GRB Coordinates Network, 1473, 1
- Li, W. D., Filippenko, A. V., & Chornock, R. 2002b, GRB Coordinates Network, 1491, 1
- Lipkin, Y. M., Ofek, E. O., Gal-Yam, A., et al. 2004, *ApJ*, 606, 381
- Littlejohns, O., Butler, N., Watson, A. M., et al. 2013a, GRB Coordinates Network, 15420, 1
- Littlejohns, O., Butler, N., Watson, A. M., et al. 2013b, GRB Coordinates Network, 15436, 1
- Littlejohns, O., Butler, N., Watson, A. M., et al. 2013c, GRB Coordinates Network, 15444, 1
- Littlejohns, O., Butler, N., Watson, A. M., et al. 2013d, GRB Coordinates Network, 15462, 1
- Littlejohns, O., Butler, N., Watson, A. M., et al. 2013e, GRB Coordinates Network, 15463, 1
- Littlejohns, O., Butler, N., Watson, A. M., et al. 2014a, GRB Coordinates Network, 16136, 1
- Littlejohns, O., Butler, N., Watson, A. M., et al. 2014b, GRB Coordinates Network, 16139, 1
- Littlejohns, O., Butler, N., Watson, A. M., et al. 2014c, GRB Coordinates Network, 16170, 1
- Litvinenko, E., Volnova, A., Molotov, I., & Pozanenko, A. 2012, GRB Coordinates Network, 13693, 1
- Loew, S., Kruehler, T., & Greiner, J. 2008, GRB Coordinates Network, 8540, 1
- Maiorano, E., Masetti, N., Palazzi, E., et al. 2006, *A&A*, 455, 423
- Malesani, D., Fugazza, D., D'Avanzo, P., et al. 2011a, GRB Coordinates Network, 11977, 1
- Malesani, D., Hjorth, J., Fynbo, J. P. U., et al. 2007, GRB Coordinates Network, 6555, 1
- Malesani, D., Leloudas, G., Xu, D., et al. 2011b, GRB Coordinates Network, 12220, 1
- Malesani, D., Piranomonte, S., Fiore, F., et al. 2005, GRB Coordinates Network, 3469, 1
- Mao, J., Cha, G., & Bai, J. 2009, GRB Coordinates Network, 9305, 1
- Margutti, R., Zaninoni, E., Bernardini, M. G., et al. 2013, *MNRAS*, 428, 729
- Martini, P., Garnavich, P., & Stanek, K. Z. 2003, GRB Coordinates Network, 1979, 1
- Maselli, A., Melandri, A., Nava, L., et al. 2014, *Science*, 343, 48
- Masi, G. & Nocentini, F. 2013, GRB Coordinates Network, 15152, 1
- McMahon, E., Kumar, P., & Piran, T. 2006, *MNRAS*, 366, 575
- Melandri, A., D'Avanzo, P., Fugazza, D., & Palazzi, E. 2011, GRB Coordinates Network, 11963, 1
- Melandri, A., Guidorzi, C., Bersier, D., et al. 2009a, GRB Coordinates Network, 9520, 1
- Melandri, A., Guidorzi, C., & Carter, D. 2008, GRB Coordinates Network, 8699, 1
- Melandri, A., Guidorzi, C., Mundell, C. G., et al. 2009b, GRB Coordinates Network, 9200, 1
- Melandri, A., Guidorzi, C., Mundell, C. G., et al. 2006, GRB Coordinates Network, 5827, 1
- Melandri, A., Japelj, J., Virgili, F. J., & Mundell, C. G. 2013a, GRB Coordinates Network, 14362, 1
- Melandri, A., Virgili, F. J., Guidorzi, C., et al. 2014, *A&A*, 572, A55
- Melandri, A., Virgili, F. J., Mundell, C. G., & Gomboc, A. 2013b, GRB Coordinates Network, 14843, 1
- Meszáros, P. & Rees, M. J. 1993, *ApJ*, 418, L59
- Milne, P. A. & Cenko, S. B. 2011, GRB Coordinates Network, 11708, 1
- Mirabal, N., Bonfield, D., & Schawinski, K. 2005, GRB Coordinates Network, 3488, 1
- Mirabal, N., McGreer, I. D., Halpern, J. P., Dietrich, M., & Peterson, B. M. 2007, GRB Coordinates Network, 6526, 1
- Misra, K., Resmi, L., Pandey, S. B., Bhattacharya, D., & Sagar, R. 2005, *Bulletin of the Astronomical Society of India*, 33, 487
- Monfardini, A., Kobayashi, S., Guidorzi, C., et al. 2006, *ApJ*, 648, 1125
- Moskvitin, A. S. 2011, GRB Coordinates Network, 11962, 1
- Moskvitin, A. S. 2013, GRB Coordinates Network, 15412, 1
- Moskvitin, A. S., Sokolov, V. V., Spiridonova, O. I., et al. 2011, GRB Coordinates Network, 12333, 1
- Mundell, C. G., Melandri, A., Guidorzi, C., et al. 2007, *ApJ*, 660, 489
- Nakajima, H., Yatsu, Y., Mori, Y. A., et al. 2009, GRB Coordinates Network, 10260, 1
- Nakar, E. & Piran, T. 2004, *MNRAS*, 353, 647
- Nakar, E. & Piran, T. 2005, *MNRAS*, 360, L73
- Narayan, R., Kumar, P., & Tchekhovskoy, A. 2011, *MNRAS*, 416, 2193
- Nardini, M., Elliott, J., Filgas, R., et al. 2014, *A&A*, 562, A29
- Nardini, M., Kruehler, T., Klose, S., Rossi, A., & Greiner, J. 2010, GRB Coordinates Network, 11337, 1
- Nava, L., Salvaterra, R., Ghirlanda, G., et al. 2012, *MNRAS*, 421, 1256
- Nevski, V., Volnova, A., Molotov, I., & Pozanenko, A. 2012, GRB Coordinates Network, 13761, 1
- Nysewander, M., Fruchter, A. S., & Pe'er, A. 2009, *ApJ*, 701, 824
- Nysewander, M., Lacluyze, A., Reichart, D., et al. 2006a, GRB Coordinates Network, 4548, 1
- Nysewander, M., Lacluyze, A., Reichart, D., et al. 2006b, GRB Coordinates Network, 4530, 1
- O Meara, J., Chen, H.-W., & Prochaska, J. X. 2010, GRB Coordinates Network, 11089, 1
- Oksanen, A. 2009, GRB Coordinates Network, 9239, 1
- Oksanen, A., Templeton, M., Henden, A. A., & Kann, D. A. 2008, *Journal of the American Association of Variable Star Observers (JAAVSO)*, 36, 53
- Olivares, E. F., Filgas, R., & Greiner, J. 2010, GRB Coordinates Network, 11013, 1
- Olivares, F., Kruehler, T., Greiner, J., & Filgas, R. 2009a, GRB Coordinates Network, 9215, 1
- Olivares, F., Kupcu Yoldas, A., Greiner, J., & Yoldas, A. 2009b, GRB Coordinates Network, 9245, 1
- Osip, D., Chen, H.-W., & Prochaska, J. X. 2006, GRB Coordinates Network, 5715, 1
- Paczynski, B. & Xu, G. 1994, *ApJ*, 427, 708
- Page, K. L., Willingale, R., Bissaldi, E., et al. 2009, *MNRAS*, 400, 134
- Pandey, S. B., Anupama, G. C., Sagar, R., et al. 2003a, *A&A*, 408, L21
- Pandey, S. B. & Kumar, B. 2014, GRB Coordinates Network, 16133, 1
- Pandey, S. B., Kumar, B., & Joshi, Y. C. 2013, GRB Coordinates Network, 15501, 1
- Pandey, S. B., Kumar, B., & Kumar, P. 2014, GRB Coordinates Network, 15677, 1
- Pandey, S. B., Sahu, D. K., Resmi, L., et al. 2003b, *Bulletin of the Astronomical Society of India*, 31, 19
- Pavlenko, E., Rumyantsev, V., & Pozanenko, A. 2009, GRB Coordinates Network, 9179, 1
- Pavlenko, E., Volnova, A., Baklanov, A., & Pozanenko, A. 2011, GRB Coordinates Network, 12005, 1
- Pélangon, A., Atteia, J.-L., Nakagawa, Y. E., et al. 2008, *A&A*, 491, 157
- Perley, D. A. 2009a, GRB Coordinates Network, 10060, 1
- Perley, D. A. 2009b, GRB Coordinates Network, 10058, 1
- Perley, D. A. 2014, GRB Coordinates Network, 16884, 1
- Perley, D. A. & Cenko, S. B. 2013, GRB Coordinates Network, 15423, 1
- Perley, D. A. & Cenko, S. B. 2014a, GRB Coordinates Network, 15674, 1
- Perley, D. A. & Cenko, S. B. 2014b, GRB Coordinates Network, 16514, 1
- Perley, D. A., Klein, C. R., & Morgan, A. N. 2010a, GRB Coordinates Network, 11025, 1
- Perley, D. A., Li, W., & Filippenko, A. V. 2010b, GRB Coordinates Network, 11024, 1
- Perley, D. A., Prochaska, J. X., & Morgan, A. N. 2012, GRB Coordinates Network, 14059, 1
- Perri, M., Barthelmy, S. D., Burrows, D. N., et al. 2009, GRB Coordinates Network, 9400, 1
- Piran, T. 1999, *Phys. Rep.*, 314, 575
- Piranomonte, S., D'Elia, V., Fiore, F., et al. 2006, GRB Coordinates Network, 4520, 1
- Pozanenko, A. 2005, GRB Coordinates Network, 4087, 1
- Price, P. A., Bloom, J. S., Goodrich, R. W., et al. 2002, GRB Coordinates Network, 1475, 1
- Price, P. A. & Fox, D. W. 2002, GRB Coordinates Network, 1732, 1
- Price, P. A., Roth, K., Rich, J., et al. 2004, GRB Coordinates Network, 2791, 1
- Prochaska, J. X., Bloom, J. S., Wright, J. T., et al. 2005, GRB Coordinates Network, 3833, 1
- Prochaska, J. X., Perley, D., Howard, A., et al. 2008, GRB Coordinates Network, 8083, 1
- Quadri, U., Strabla, L., Girelli, R., & Quadri, A. 2012, GRB Coordinates Network, 13178, 1
- Rees, M. J. & Meszáros, P. 1994, *ApJ*, 430, L93
- Rees, M. J. & Mészáros, P. 2005, *ApJ*, 628, 847
- Resmi, L., Misra, K., Jóhannesson, G., et al. 2012, *MNRAS*, 427, 288
- Rol, E., Vreeswijk, P., & Jaunsen, A. 2003, GRB Coordinates Network, 1981, 1
- Rossi, A., Afonso, P., & Greiner, J. 2009a, GRB Coordinates Network, 9382, 1
- Rossi, A., Kruehler, T., Greiner, J., & Yoldas, A. 2009b, GRB Coordinates Network, 9408, 1
- Roy, R., Kumar, B., Pandey, S. B., & Kumar, B. 2008, GRB Coordinates Network, 8717, 1
- Roy, R., Kumar, B., Pandey, S. B., & Kumar, B. 2009, GRB Coordinates Network, 9278, 1
- Rujopakarn, W., Guver, T., Pandey, S. B., & Yuan, F. 2009, GRB Coordinates

- Network, 9515, 1
- Rujopakarn, W. & Rykoff, E. S. 2008, GRB Coordinates Network, 8056, 1
- Rujopakarn, W., Schaefer, B. E., & Rykoff, E. S. 2011, GRB Coordinates Network, 11707, 1
- Rumyantsev, V., Antoniuk, K., & Pozanenko, A. 2009, GRB Coordinates Network, 9320, 1
- Rumyantsev, V., Antoniuk, K., & Pozanenko, A. 2011a, GRB Coordinates Network, 11973, 1
- Rumyantsev, V., Biryukov, V., & Pozanenko, A. 2003, GRB Coordinates Network, 1991, 1
- Rumyantsev, V., Biryukov, V., & Pozanenko, A. 2005, GRB Coordinates Network, 4081, 1
- Rumyantsev, V. & Pozanenko, A. 2008, GRB Coordinates Network, 7857, 1
- Rumyantsev, V. & Pozanenko, A. 2009, GRB Coordinates Network, 9539, 1
- Rumyantsev, V. & Pozanenko, A. 2013, GRB Coordinates Network, 14907, 1
- Rumyantsev, V., Pozanenko, A., & Klunko, E. 2011b, GRB Coordinates Network, 11986, 1
- Rykoff, E. S. & Rujopakarn, W. 2008, GRB Coordinates Network, 7593, 1
- Rykoff, E. S., Yost, S. A., & Swan, H. 2005, GRB Coordinates Network, 3465, 1
- Rykoff, K. & BenDaniel, M. 2005, GRB Coordinates Network, 3470, 1
- Sahu, D. K. 2014, GRB Coordinates Network, 16272, 1
- Sahu, D. K., Anupama, G. C., & Pandey, S. B. 2012, GRB Coordinates Network, 13185, 1
- Sahu, K. C., Vreeswijk, P., Bakos, G., et al. 2000, *ApJ*, 540, 74
- Sakamoto, T., Barbier, L., Barthelmy, S. D., et al. 2006, *ApJ*, 636, L73
- Sanchez-Ramirez, R., Gorosabel, J., de Ugarte Postigo, A., & Gonzalez Perez, J. M. 2012, GRB Coordinates Network, 13723, 1
- Sari, R., Piran, T., & Narayan, R. 1998, *ApJ*, 497, L17
- Schady, P., de Pasquale, M., Page, M. J., et al. 2007a, *MNRAS*, 380, 1041
- Schady, P., Mason, K. O., Page, M. J., et al. 2007b, *MNRAS*, 377, 273
- Schady, P., Page, M. J., Oates, S. R., et al. 2010, *MNRAS*, 401, 2773
- Schaefer, B. E. & Collazzi, A. C. 2007, *ApJ*, 656, L53
- Schaefer, B. E., McKay, T. A., & Yuan, F. 2007, GRB Coordinates Network, 6948, 1
- Schlegel, D. J., Finkbeiner, D. P., & Davis, M. 1998, *ApJ*, 500, 525
- Schmidl, S., Graham, J. F., & Greiner, J. 2014, GRB Coordinates Network, 16898, 1
- Schulze, S., Wiersema, K., Xu, D., & Fynbo, J. P. U. 2014, GRB Coordinates Network, 15831, 1
- Shahmoradi, A. 2013, ArXiv e-prints
- Shahmoradi, A. & Nemiroff, R. J. 2011, *MNRAS*, 411, 1843
- Singer, L. P., Kasliwal, M. M., Cenko, S. B., et al. 2015, ArXiv e-prints
- Smette, A., Ledoux, C., Vreeswijk, P., et al. 2013, GRB Coordinates Network, 14848, 1
- Smith, R. J., Gomboc, A., Guidorzi, C., et al. 2009a, GRB Coordinates Network, 9770, 1
- Smith, R. J., Steele, I. A., Cano, Z., et al. 2009b, GRB Coordinates Network, 9784, 1
- Soderberg, A. M., Kulkarni, S. R., Price, P. A., et al. 2006, *ApJ*, 636, 391
- Sonbas, E., Temiz, U., Guver, T., et al. 2013, GRB Coordinates Network, 15161, 1
- Sonoda, E., Tanaka, H., Hara, R., et al. 2008, GRB Coordinates Network, 8697, 1
- Soulier, J.-F. 2012, GRB Coordinates Network, 13126, 1
- Stanek, K. Z., Garnavich, P. M., Nutzman, P. A., et al. 2005, *ApJ*, 626, L5
- Starling, R. L. C., Rol, E., van der Horst, A. J., et al. 2009, *MNRAS*, 400, 90
- Sudilovsky, V., Nicuesa Guelbenzu, A., & Greiner, J. 2013, GRB Coordinates Network, 14364, 1
- Tanga, M., Graham, J. F., Kann, D. A., & Greiner, J. 2014a, GRB Coordinates Network, 16458, 1
- Tanga, M., Klose, S., & Greiner, J. 2014b, GRB Coordinates Network, 15665, 1
- Tanigawa, T., Yoshii, T., Ito, K., et al. 2013, GRB Coordinates Network, 15481, 1
- Tanvir, N. R., Fox, D. B., Levan, A. J., et al. 2009, *Nature*, 461, 1254
- Tanvir, N. R., Levan, A. J., Cucchiara, A., Perley, D., & Cenko, S. B. 2014a, GRB Coordinates Network, 16125, 1
- Tanvir, N. R., Levan, A. J., Matulonis, T., & Smith, A. B. 2013, GRB Coordinates Network, 14567, 1
- Tanvir, N. R., Levan, A. J., Wiersema, K., et al. 2014b, GRB Coordinates Network, 16150, 1
- Tanvir, N. R., Wiersema, K., Levan, A. J., Cenko, S. B., & Geballe, T. 2011, GRB Coordinates Network, 12225, 1
- Tasselli, A. 2011, GRB Coordinates Network, 12014, 1
- Tello, J. C., Jelinek, M., Castro-Tirado, A. J., et al. 2010, GRB Coordinates Network, 11343, 1
- Tello, J. C., Sanchez-Ramirez, R., Gorosabel, J., et al. 2012, GRB Coordinates Network, 13118, 1
- Terron, V., Fernandez, M., & Gorosabel, J. 2013, GRB Coordinates Network, 15411, 1
- Testa, V., Fugazza, D., Della Valle, M., et al. 2003, GRB Coordinates Network, 1821, 1
- Thoene, C. C., De Cia, A., Malesani, D., & Vreeswijk, P. M. 2008a, GRB Coordinates Network, 7587, 1
- Thoene, C. C., de Ugarte Postigo, A., Gorosabel, J., et al. 2012, GRB Coordinates Network, 13628, 1
- Thoene, C. C., Goldoni, P., Covino, S., et al. 2009a, GRB Coordinates Network, 10233, 1
- Thoene, C. C., Jakobsson, P., De Cia, A., et al. 2009b, GRB Coordinates Network, 9409, 1
- Thoene, C. C., Malesani, D., Levan, A. J., et al. 2009c, GRB Coordinates Network, 9403, 1
- Thoene, C. C., Malesani, D., Vreeswijk, P. M., et al. 2008b, GRB Coordinates Network, 7602, 1
- Thöne, C. C., Greiner, J., Savaglio, S., & Jehin, E. 2007, *ApJ*, 671, 628
- Toma, K., Yamazaki, R., & Nakamura, T. 2005, *ApJ*, 635, 481
- Troja, E., Sakamoto, T., Guidorzi, C., et al. 2012, *ApJ*, 761, 50
- Trotter, A., Frank, N., Lacluyze, A., et al. 2013a, GRB Coordinates Network, 14375, 1
- Trotter, A., Frank, N., Lacluyze, A., et al. 2013b, GRB Coordinates Network, 14445, 1
- Trotter, A., Haislip, J., Reichart, D., et al. 2014, GRB Coordinates Network, 15859, 1
- Uemura, M., Arai, A., & Uehara, T. 2006, GRB Coordinates Network, 5828, 1
- Ukwatta, T. N., Sonbas, E., Gehrels, N., et al. 2011, GRB Coordinates Network, 11715, 1
- Utdike, A., Brittain, S., Hartmann, D., et al. 2009a, GRB Coordinates Network, 9529, 1
- Utdike, A., Rau, A., Kruehler, T., Olivares, F., & Greiner, J. 2009b, GRB Coordinates Network, 9773, 1
- Utdike, A., Rossi, A., & Greiner, J. 2009c, GRB Coordinates Network, 10271, 1
- Utdike, A. C., Hartmann, D. H., Henson, G., et al. 2007a, GRB Coordinates Network, 6515, 1
- Utdike, A. C., Kann, D. A., Hartmann, D. H., & Rumstay, K. 2011, GRB Coordinates Network, 12001, 1
- Utdike, A. C., Milne, P. A., Williams, G. G., & Hartmann, D. H. 2007b, GRB Coordinates Network, 6535, 1
- Utdike, A. C., Puls, J., Hartmann, D. H., et al. 2007c, GRB Coordinates Network, 6530, 1
- Urata, J. 2006a, GRB Coordinates Network, 5547, 1
- Urata, J. 2006b, GRB Coordinates Network, 4430, 1
- Urata, Y., Huang, K. Y., Qiu, Y. L., et al. 2007, *ApJ*, 655, L81
- Urata, Y., Nishiura, S., Miyata, T., et al. 2003, *ApJ*, 595, L21
- Urata, Y., Zhang, Z. W., Wen, C. Y., Huang, K. Y., & Wang, S. Y. 2009, GRB Coordinates Network, 9240, 1
- Vaalsta, T. P., Coward, D. M., Ward, I., et al. 2009a, GRB Coordinates Network, 10238, 1
- Vaalsta, T. P., Yan, L., Zadko, J., et al. 2009b, GRB Coordinates Network, 9380, 1
- Vestrand, W. T., Wren, J. A., Panaitescu, A., et al. 2014, *Science*, 343, 38
- Virgili, F. J., Mundell, C. G., Japelj, J., et al. 2013, GRB Coordinates Network, 15406, 1
- Volnova, A., Inasaridze, R., Inasaridze, G., et al. 2014a, GRB Coordinates Network, 15730, 1
- Volnova, A., Inasaridze, R., Kvaratskhelia, O., et al. 2014b, GRB Coordinates Network, 16264, 1
- Volnova, A., Inasaridze, R., Kvaratskhelia, O., et al. 2014c, GRB Coordinates Network, 16536, 1
- Volnova, A., Klunko, E., Eselevich, M., Korobtsev, I., & Pozanenko, A. 2014d, GRB Coordinates Network, 16168, 1
- Volnova, A., Klunko, E., Eselevich, M., Korobtsev, I., & Pozanenko, A. 2014e, GRB Coordinates Network, 16247, 1
- Volnova, A., Kusakin, A. V., Khruslov, A. V., & Pozanenko, A. 2014f, GRB Coordinates Network, 16318, 1
- Volnova, A., Linkov, V., Polyakov, K., et al. 2013a, GRB Coordinates Network, 15188, 1
- Volnova, A., Matkin, A., Stepura, A., Molotov, I., & Pozanenko, A. 2013b, GRB Coordinates Network, 15185, 1
- Volnova, A., Minikulov, N., Gulyamov, M., Molotov, I., & Pozanenko, A. 2013c, GRB Coordinates Network, 15186, 1
- Volnova, A., Mundrzyjewski, W., Kusakin, A., & Pozanenko, A. 2014g, GRB Coordinates Network, 16651, 1
- Volnova, A., Pavlenko, E., Antoniuk, O., Rumyantsev, V., & Pozanenko, A. 2009, GRB Coordinates Network, 9811, 1
- Volnova, A., Pozanenko, A., Korobtsev, I., & Elunko, E. 2011, GRB Coordinates

- Network, 11742, 1
- Volnova, A., Schmalz, S., Tungalag, N., et al. 2014h, GRB Coordinates Network, 16558, 1
- Volnova, A. A., Pozanenko, A. S., Gorosabel, J., et al. 2014i, MNRAS, 442, 2586
- Vreeswijk, P. M., Galama, T. J., Rol, E., et al. 1999, GRB Coordinates Network, 324, 1
- Vreeswijk, P. M., Milvang-Jensen, B., Smette, A., et al. 2008a, GRB Coordinates Network, 7451, 1
- Vreeswijk, P. M., Thoene, C. C., Malesani, D., et al. 2008b, GRB Coordinates Network, 7601, 1
- Wang, J. H., Schwamb, M. E., Huang, K. Y., et al. 2008, ApJ, 679, L5
- Watson, A. M., Butler, N., Kutyrev, A., et al. 2013a, GRB Coordinates Network, 14439, 1
- Watson, A. M., Butler, N., Kutyrev, A., et al. 2013b, GRB Coordinates Network, 14595, 1
- Watson, A. M., Littlejohns, O., Butler, N., et al. 2013c, GRB Coordinates Network, 15179, 1
- Wiersema, K., Tanvir, N. R., Cucchiara, A., Levan, A. J., & Fox, D. 2009, GRB Coordinates Network, 10263, 1
- Wiersema, K., van der Horst, A. J., Kann, D. A., et al. 2008, A&A, 481, 319
- Williams, G. G., Blake, C., Hartmann, D., & S-LOTIS collaboration. 2002, GRB Coordinates Network, 1492, 1
- Woźniak, P. R., Vestrand, W. T., Panaitescu, A. D., et al. 2009, ApJ, 691, 495
- Woźniak, P. R., Vestrand, W. T., Wren, J. A., et al. 2006, ApJ, 642, L99
- Wren, J., Vestrand, W. T., Woźniak, P. R., & Davis, H. 2011, GRB Coordinates Network, 11730, 1
- Wren, J., Vestrand, W. T., Woźniak, P. R., Davis, H., & Norman, B. 2009, GRB Coordinates Network, 9778, 1
- Xiao, L. & Schaefer, B. E. 2009, ApJ, 707, 387
- Xin, L., Liu, H., Qiu, Y., et al. 2010, GRB Coordinates Network, 10583, 1
- Xin, L. P., Han, X. H., Qiu, Y. L., et al. 2013a, GRB Coordinates Network, 15146, 1
- Xin, L. P., Qian, S. B., Qiu, Y. L., et al. 2009a, GRB Coordinates Network, 10279, 1
- Xin, L. P., Wang, X. F., Wang, J., et al. 2009b, GRB Coordinates Network, 10080, 1
- Xin, L. P., Wei, J. Y., Qiu, Y. L., et al. 2013b, GRB Coordinates Network, 15425, 1
- Xin, L. P., Wei, J. Y., Qiu, Y. L., et al. 2012a, GRB Coordinates Network, 13149, 1
- Xin, L. P., Wei, J. Y., Qiu, Y. L., et al. 2012b, GRB Coordinates Network, 13131, 1
- Xin, L. P., Wei, J. Y., Qiu, Y. L., et al. 2013c, GRB Coordinates Network, 14571, 1
- Xin, L. P., Yan, J. Z., Wei, J. Y., et al. 2014, GRB Coordinates Network, 16586, 1
- Xu, D. 2014, GRB Coordinates Network, 16140, 1
- Xu, D., Cao, C., Hu, S.-M., & Ai, J.-M. 2013a, GRB Coordinates Network, 14570, 1
- Xu, D., de Ugarte Postigo, A., Malesani, D., et al. 2013b, GRB Coordinates Network, 14956, 1
- Xu, D., Fynbo, J. P. U., Jakobsson, P., et al. 2013c, GRB Coordinates Network, 15407, 1
- Xu, D., Fynbo, J. P. U., Nielsen, M., & Jakobsson, P. 2011a, GRB Coordinates Network, 11970, 1
- Xu, D., Fynbo, J. P. U., Tanvir, N. R., et al. 2009a, GRB Coordinates Network, 10053, 1
- Xu, D., Kankare, E., Kangas, T., & Jakobsson, P. 2011b, GRB Coordinates Network, 11974, 1
- Xu, D., Leloudas, G., Malesani, D., et al. 2009b, GRB Coordinates Network, 10269, 1
- Xu, D., Malesani, D., Hjorth, J., et al. 2009c, GRB Coordinates Network, 10196, 1
- Xu, D., Zhang, C. M., Cao, C., & Hu, S. M. 2013d, GRB Coordinates Network, 15142, 1
- Xu, D., Zhang, X., Bai, C.-H., et al. 2014, GRB Coordinates Network, 15655, 1
- Yanagisawa, K., Toda, H., & Kawai, N. 2005, GRB Coordinates Network, 3489, 1
- Yanagisawa, K., Toda, H., & Kawai, N. 2006, GRB Coordinates Network, 4517, 1
- Yoshida, M., Kuroda, D., Yanagisawa, K., et al. 2009a, GRB Coordinates Network, 10258, 1
- Yoshida, M., Yanagisawa, K., Kuroda, D., et al. 2008a, GRB Coordinates Network, 7863, 1
- Yoshida, M., Yanagisawa, K., Kuroda, D., et al. 2008b, GRB Coordinates Network, 8097, 1
- Yoshida, M., Yanagisawa, K., Kuroda, D., et al. 2009b, GRB Coordinates Network, 9218, 1
- Yoshii, T., Ito, K., Saito, Y., et al. 2013, GRB Coordinates Network, 15143, 1
- Yoshii, T., Saito, Y., Kurita, S., et al. 2014, GRB Coordinates Network, 15778, 1
- Yost, S. A., Schaefer, B. E., & Yuan, F. 2006, GRB Coordinates Network, 5824, 1
- Yuan, F. 2009, GRB Coordinates Network, 9224, 1
- Yuan, F. & Rujopakarn, W. 2008, GRB Coordinates Network, 8536, 1
- Yuan, F. & Rujopakarn, W. 2009, GRB Coordinates Network, 9150, 1
- Yuan, F., Schady, P., Racusin, J. L., et al. 2010, ApJ, 711, 870
- Zafar, T., Watson, D., Elíasdóttir, Á., et al. 2012, ApJ, 753, 82
- Zhang, B. & Kobayashi, S. 2005, ApJ, 628, 315
- Zhao, X. H., Bai, J. M., & Mao, J. 2011, GRB Coordinates Network, 11733, 1
- Zhao, X.-H., Mao, J., & Bai, J.-M. 2013, GRB Coordinates Network, 14418, 1
- Zhao, X.-H., Mao, J., Xu, D., & Bai, J.-M. 2012, GRB Coordinates Network, 13122, 1
- Zheng, W., Filippenko, A. V., Morgan, A., & Cenko, S. B. 2014, GRB Coordinates Network, 16137, 1
- Zheng, W., Shen, R. F., Sakamoto, T., et al. 2012, ApJ, 751, 90
- Zheng, W., Yuan, F., & Pandey, S. B. 2009, GRB Coordinates Network, 10284, 1
- Zimmerman, N. & Tyagi, S. 2006, GRB Coordinates Network, 4440, 1



**Table 7.** Table of references**References for the afterglow optical light curve**

- (1) Kulkarni et al. (1999), (2) Harrison et al. (1999), (3) Sahu et al. (2000), (4) Berger et al. (2002)  
 (5) Hjorth et al. (2003), (6) Urata et al. (2003), (7) Laursen & Stanek (2003), (8) Li et al. (2002a)  
 (9) Li et al. (2002b), (10) Williams et al. (2002), (11) Beskin et al. (2002), (12) Kiziloglu et al. (2002)  
 (13) Fiore et al. (2002), (14) Gorosabel et al. (2002), (15) Pandey et al. (2003b), (16) Holland et al. (2003)  
 (17) Bersier et al. (2003), (18) de Ugarte Postigo et al. (2005), (19) Garnavich & Quinn (2002), (20) Fox et al. (2003)  
 (21) Li et al. (2003), (22) Holland et al. (2004), (23) Pandey et al. (2003a), (24) Testa et al. (2003)  
 (25) Price & Fox (2002), (26) Maiorano et al. (2006), (27) Burenin et al. (2003), (28) Rumyantsev et al. (2003)  
 (29) Fugazza et al. (2003), (30) Ibrahimov et al. (2003), (31) Martini et al. (2003), (32) Gorosabel et al. (2006)  
 (33) Lipkin et al. (2004), (34) Huang et al. (2005), (35) Soderberg et al. (2006), (36) Wiersema et al. (2008)  
 (37) Stanek et al. (2005), (38) Urata et al. (2007), (39) Misra et al. (2005), (40) Kann et al. (2010)  
 (41) Resmi et al. (2012), (42) Klotz et al. (2005), (43) Rykoff et al. (2005), (44) Rykoff & BenDaniel (2005)  
 (45) Malesani et al. (2005), (46) Mirabal et al. (2005), (47) Cobb & Baily (2005), (48) Durig et al. (2005)  
 (49) Haislip et al. (2005), (50) Yanagisawa et al. (2005), (51) Kann et al. (2010), (52) Cenko et al. (2006)  
 (53) Kann et al. (2010), (54) Kann et al. (2010), (55) Yanagisawa et al. (2006), (56) Distefano et al. (2006)  
 (57) Nysewander et al. (2006b), (58) Covino et al. (2010), (59) Mundell et al. (2007), (60) Kann et al. (2010)  
 (61) Halpern et al. (2006), (62) Halpern & Armstrong (2006b), (63) Halpern & Armstrong (2006a)  
 (64) Yost et al. (2006), (65) Melandri et al. (2006), (66) Uemura et al. (2006), (67) Urdike et al. (2007a)  
 (68) Urdike et al. (2007c), (69) Urdike et al. (2007b), (70) Mirabal et al. (2007), (71) Malesani et al. (2007)  
 (72) Lee et al. (2010), (73) Oksanen et al. (2008), (74) Wang et al. (2008), (75) Kann et al. (2007)  
 (76) Kocevski et al. (2007), (77) Kann et al. (2010), (78) Schaefer et al. (2007), (79) Ishimura et al. (2007)  
 (80) Hentunen (2007), (81) Im et al. (2007), (82) Bloom et al. (2009), (83) Woźniak et al. (2009)  
 (84) Kruehler et al. (2008a), (85) Thoene et al. (2008a), (86) Kann et al. (2010), (87) Rykoff & Rujopakarn (2008)  
 (88) Gomboc et al. (2008a), (89) Cobb (2008a), (90) Klotz et al. (2008), (91) Brennan et al. (2008)  
 (92) Gomboc et al. (2008b), (93) Zafar et al. (2012), (94) Kuvshinov et al. (2008), (95) Rumyantsev & Pozanenko (2008)  
 (96) Gomboc et al. (2008c), (97) Kann et al. (2008), (98) Jakobsson et al. (2008b), (99) Yoshida et al. (2008a)  
 (100) Starling et al. (2009), (101) Chen et al. (2008), (102) Huang et al. (2008), (103) Rujopakarn & Rykoff (2008)  
 (104) Kruehler et al. (2008b), (105) Guidorzi & Steele (2008), (106) Page et al. (2009), (107) Kann et al. (2010)  
 (108) Yoshida et al. (2008b), (109) Jin et al. (2013), (110) Yuan et al. (2010), (111) Cobb (2008b)  
 (112) Kann et al. (2010), (113) Cucchiara et al. (2008a), (114) Yuan & Rujopakarn (2008), (115) Loew et al. (2008)  
 (116) Cobb (2008c), (117) Covino et al. (2013), (118) Cwiok et al. (2008), (119) Sonoda et al. (2008)  
 (120) Kuroda et al. (2008), (121) Melandri et al. (2008), (122) Roy et al. (2008), (123) Gendre et al. (2010)  
 (124) Yuan & Rujopakarn (2009), (125) Henden et al. (2009b), (126) Chornock et al. (2009b), (127) Bikmaev et al. (2009)  
 (128) Pavlenko et al. (2009), (129) Henden et al. (2009a), (130) Cenko (2009a), (131) Melandri et al. (2009b)  
 (132) Yoshida et al. (2009b), (133) Olivares et al. (2009a), (134) Kann et al. (2010), (135) Jin et al. (2013)  
 (136) Urata et al. (2009), (137) Yuan (2009), (138) Mao et al. (2009), (139) Roy et al. (2009)  
 (140) Rumyantsev et al. (2009), (141) Oksanen (2009), (142) Gorosabel et al. (2009b), (143) Olivares et al. (2009b)  
 (144) Im et al. (2009a), (145) Guidorzi et al. (2009), (146) Christie et al. (2009a), (147) Vaalsta et al. (2009b)  
 (148) Gorosabel et al. (2009a), (149) de Ugarte Postigo et al. (2009c), (150) Rossi et al. (2009a), (151) Klotz et al. (2009a)  
 (152) Klotz & Kugel (2009), (153) Jelinek & Kubanek (2009), (154) Rossi et al. (2009b), (155) Thoene et al. (2009c)  
 (156) Thoene et al. (2009b), (157) Rujopakarn et al. (2009), (158) Li et al. (2009), (159) Cenko (2009b)  
 (160) Im et al. (2009b), (161) Urdike et al. (2009a), (162) Melandri et al. (2009a), (163) Klunko et al. (2009)  
 (164) Anumapa et al. (2009), (165) Rumyantsev & Pozanenko (2009), (166) Cano et al. (2009a), (167) Fernandez-Soto et al. (2009)  
 (168) Fatkhullin et al. (2009), (169) Galeev et al. (2009), (170) Khamitov et al. (2009), (171) Wren et al. (2009)  
 (172) Smith et al. (2009a), (173) Haislip et al. (2009a), (174) Urdike et al. (2009b), (175) Gorbvskoy et al. (2009)  
 (176) Kann et al. (2009a), (177) Kann et al. (2009b), (178) Xu et al. (2009a), (179) Perley (2009b)  
 (180) Perley (2009a), (181) Xin et al. (2009b), (182) Filgas et al. (2009b), (183) Chornock et al. (2009d)  
 (184) Christie et al. (2009b), (185) de Ugarte Postigo et al. (2009a), (186) Troja et al. (2012), (187) Filgas et al. (2011)  
 (188) Xu et al. (2009c), (189) Klotz et al. (2009b), (190) Cobb et al. (2010), (191) Kinugasa et al. (2009a)  
 (192) Vaalsta et al. (2009a), (193) Andreev et al. (2009b), (194) Haislip et al. (2009b), (195) Haislip et al. (2009c)  
 (196) Thoene et al. (2009a), (197) Nakajima et al. (2009), (198) Cano et al. (2009b), (199) Yoshida et al. (2009a)  
 (200) Xin et al. (2009a), (201) Kinugasa et al. (2009b), (202) Andreev et al. (2009a), (203) Xu et al. (2009b)  
 (204) Urdike et al. (2009c), (205) Perley et al. (2010b), (206) Perley et al. (2010a), (207) Elenin et al. (2010)  
 (208) De Cia et al. (2010), (209) Olivares et al. (2010), (210) Nardini et al. (2014), (211) Zheng et al. (2012)  
 (212) Gendre et al. (2012), (213) Cucchiara et al. (2011a), (214) Cucchiara et al. (2011a), (215) Rujopakarn et al. (2011)  
 (216) Wren et al. (2011), (217) Ukwatta et al. (2011), (218) Hentunen et al. (2011a), (219) Kuroda et al. (2011c)  
 (220) Volnova et al. (2011), (221) Zhao et al. (2011), (222) Hentunen et al. (2011c), (223) Elunko & Pozanenko (2011)  
 (224) Moskvitin (2011), (225) Rumyantsev et al. (2011a), (226) Hentunen et al. (2011b), (227) Xu et al. (2011a)  
 (228) Melandri et al. (2011), (229) Jeon et al. (2011), (230) Kuroda et al. (2011a), (231) Xu et al. (2011b)  
 (232) Rumyantsev et al. (2011b), (233) Klotz et al. (2011), (234) Kann et al. (2011), (235) Leloudas et al. (2011)

**Table 7.** continued

- (236) Tasselli (2011), (237) Broens & Boyd (2011), (238) D’Avanzo et al. (2011), (239) Pavlenko et al. (2011)  
 (240) Im et al. (2011), (241) Utdike et al. (2011), (242) Bersier (2011), (243) Kuroda et al. (2011b)  
 (244) Moskvitin et al. (2011), (245) Malesani et al. (2011b), (246) Tanvir et al. (2011), (247) Ackermann et al. (2013)  
 (248) Melandri et al. (2014), (249) Klotz et al. (2012), (250) Hentunen et al. (2012), (251) Jang et al. (2012)  
 (252) Zhao et al. (2012), (253) Xin et al. (2012b), (254) Xin et al. (2012a), (255) Soulier (2012)  
 (256) Quadri et al. (2012), (257) Sahu et al. (2012), (258) Elenin et al. (2012), (259) Litvinenko et al. (2012)  
 (260) Galeev et al. (2012a), (261) Galeev et al. (2012b), (262) Nevski et al. (2012), (263) Japelj et al. (2012)  
 (264) Kuroda et al. (2012), (265) Butler et al. (2012a), (266) Butler et al. (2012b), (267) Melandri et al. (2013a)  
 (268) Sudilovsky et al. (2013), (269) Trotter et al. (2013a), (270) Dereli et al. (2013), (271) Guver (2013)  
 (272) Elenin et al. (2013b), (273) Guidorzi et al. (2013), (274) Trotter et al. (2013b), (275) Hentunen et al. (2013a)  
 (276) Butler et al. (2013a), (277) Watson et al. (2013a), (278) Butler et al. (2013b), (279) Zhao et al. (2013)  
 (280) Vestrand et al. (2014), (281) Maselli et al. (2014), (282) Hentunen et al. (2013b), (283) Kuroda et al. (2013)  
 (284) Xu et al. (2013a), (285) Xin et al. (2013c), (286) Kann et al. (2013), (287) Krugly et al. (2013)  
 (288) Watson et al. (2013b), (289) Klotz et al. (2013), (290) Melandri et al. (2013b), (291) Hentunen & Nissinen (2013)  
 (292) Elenin et al. (2013a), (293) Cenko & Perley (2013a), (294) Im et al. (2013), (295) Rummyantsev & Pozanenko (2013)  
 (296) Leloudas et al. (2013), (297) Cenko & Perley (2013b), (298) Xu et al. (2013b), (299) Cano et al. (2014a)  
 (300) Yoshii et al. (2013), (301) Guidorzi & Melandri (2013), (302) Volnova et al. (2013b), (303) Xu et al. (2013d)  
 (304) Izzo & D’Avino (2013), (305) Xin et al. (2013a), (306) Sonbas et al. (2013), (307) Volnova et al. (2013c)  
 (308) Volnova et al. (2013a), (309) Hentunen et al. (2013d), (310) Leonini et al. (2013), (311) Khorunzhev et al. (2013)  
 (312) Masi & Nocentini (2013), (313) Butler et al. (2013c), (314) Watson et al. (2013c), (315) Lee et al. (2013)  
 (316) Moskvitin (2013), (317) Xu et al. (2013c), (318) Virgili et al. (2013), (319) Gorbvskoy et al. (2013)  
 (320) Terron et al. (2013), (321) Im & Choi (2013), (322) Perley & Cenko (2013), (323) Littlejohns et al. (2013a)  
 (324) Littlejohns et al. (2013b), (325) Littlejohns et al. (2013c), (326) Littlejohns et al. (2013d), (327) Littlejohns et al. (2013e)  
 (328) Hentunen et al. (2013c), (329) Tanigawa et al. (2013), (330) Xin et al. (2013b), (331) Pandey et al. (2013)  
 (332) Trotter et al. (2014), (333) Elliott et al. (2014), (334) Guver et al. (2014), (335) Zheng et al. (2014)  
 (336) Butler et al. (2014a), (337) Littlejohns et al. (2014a), (338) Littlejohns et al. (2014b), (339) Cenko & Perley (2014a)  
 (340) Hentunen et al. (2014), (341) Choi et al. (2014a), (342) Kuroda et al. (2014b), (343) Kuroda et al. (2014a)  
 (344) Volnova et al. (2014d), (345) Pandey & Kumar (2014), (346) Xu (2014), (347) Ferrante et al. (2014)  
 (348) Elenin et al. (2014), (349) Cenko & Perley (2014b), (350) Harbeck et al. (2014a), (351) Harbeck et al. (2014b)  
 (352) Akitaya et al. (2014), (353) Kuroda et al. (2014c), (354) Fujiwara et al. (2014), (355) Volnova et al. (2014f)  
 (356) Sahu (2014), (357) Cano et al. (2014b), (358) Volnova et al. (2014b), (359) Bikmaev et al. (2014)  
 (360) Littlejohns et al. (2014c), (361) Butler et al. (2014b), (362) Volnova et al. (2014e), (363) Fynbo et al. (2014)  
 (364) Gorbvskoy et al. (2014), (365) Klunko et al. (2014), (366) de Ugarte Postigo et al. (2014a), (367) Graham et al. (2014)  
 (368) Ciabattari et al. (2014), (369) Perley & Cenko (2014b), (370) Butler et al. (2014c), (371) Volnova et al. (2014c)  
 (372) Rummyantsev et al. (2005), (373) Pozanenko (2005), (374) Volnova et al. (2014i), (375) Urata (2006b)  
 (376) Zimmerman & Tyagi (2006), (377) Kann & Manohar (2006), (378) Nysewander et al. (2006a), (379) Klotz et al. (2006)  
 (380) Cenko & Rau (2006), (381) Urata (2006a), (382) Smith et al. (2009b), (383) Volnova et al. (2009)  
 (384) Zheng et al. (2009), (385) Filgas et al. (2009a), (386) Haislip et al. (2009d), (387) Ivanov et al. (2010)  
 (388) Guidorzi et al. (2010), (389) Xin et al. (2010), (390) Filgas et al. (2010), (391) Laas-Bourez et al. (2010)  
 (392) Nardini et al. (2010), (393) de Pasquale & Cannizzo (2010), (394) Tello et al. (2010), (395) Yoshii et al. (2014)  
 (396) Guziy et al. (2014), (397) Chen et al. (2014), (398) Xu et al. (2014), (399) Pandey et al. (2014)  
 (400) Tanga et al. (2014b), (401) Perley & Cenko (2014a), (402) Choi et al. (2014b), (403) Volnova et al. (2014a)  
 (404) Klotz et al. (2014a), (405) Tanga et al. (2014a), (406) Ivanov et al. (2014), (407) Volnova et al. (2014h)  
 (408) Volnova et al. (2014g), (409) Xin et al. (2014), (410) Cano et al. (2014b), (411) Perley (2014)  
 (412) Schmidl et al. (2014), (413) Klotz et al. (2014b), (414) Kann et al. (2014)

**Table 7.** continued

<b>References for the redshift</b>	
A. Kulkarni et al. (1999), B. Vreeswijk et al. (1999), C. Galama et al. (1999), D. Hjorth et al. (2003) E. Price et al. (2002), F. Castro-Tirado et al. (2010), G. Della Valle et al. (2003), H. Rol et al. (2003) I. Thöne et al. (2007), J. Wiersema et al. (2008), K. Price et al. (2004), L. Cenko et al. (2005) M. Foley et al. (2005), N. Prochaska et al. (2005), O. Jakobsson et al. (2005), P. Piranomonte et al. (2006) Q. Fynbo et al. (2009), R. Osip et al. (2006), S. Bloom et al. (2006), T. Cenko et al. (2007b) U. Cenko et al. (2007a), V. Jakobsson et al. (2007), W. Vreeswijk et al. (2008a), X. Thoene et al. (2008a) Y. Thoene et al. (2008b), Z. Vreeswijk et al. (2008b), AA. Jakobsson et al. (2008b), AB. Jakobsson et al. (2008a) AC. Cucchiara et al. (2008d), AD. Prochaska et al. (2008), AE. Berger et al. (2008), AF. Cucchiara et al. (2008b) AG. Berger & Rauch (2008), AH. Cucchiara et al. (2008c), AI. Cucchiara & Fox (2009), AJ. Chornock et al. (2009a) AK. Tanvir et al. (2009), AL. Chornock et al. (2009c), AM. de Ugarte Postigo et al. (2009d), AN. Thoene et al. (2009b) AO. Cenko et al. (2009), AP. de Ugarte Postigo et al. (2009b), AQ. Xu et al. (2009a), AR. Chornock et al. (2009d) AS. Cucchiara et al. (2009), AT. Wiersema et al. (2009), AU. Flores et al. (2010), AV. O Meara et al. (2010) AW. Cenko et al. (2011), AX. Milne & Cenko (2011), AY. Malesani et al. (2011a), AZ. de Ugarte Postigo et al. (2011) BA. Tanvir et al. (2011), BB. Tello et al. (2012), BC. Thoene et al. (2012), BD. Sanchez-Ramirez et al. (2012) BE. Perley et al. (2012), BF. Hjorth et al. (2013), BG. de Ugarte Postigo et al. (2013), BH. Flores et al. (2013) BI. Tanvir et al. (2013), BJ. Smette et al. (2013), BK. Xu et al. (2013b), BL. Cucchiara & Perley (2013) BM. Xu et al. (2013c), BN. Schulze et al. (2014), BO. Tanvir et al. (2014a), BP. Tanvir et al. (2014b) BQ. Fynbo et al. (2014), BR. de Ugarte Postigo et al. (2014b), BS. Castro-Tirado et al. (2014)	
<b>References for the host extinction</b>	
a) Japelj et al. (2014), b) Christensen et al. (2004), c) Schady et al. (2007b), d) Kann et al. (2010) e) Schady et al. (2010), f) Schady et al. (2007a), g) Greiner et al. (2011)	